Takuro Michibata
Research Institute for Applied Mechanics
Kyushu University
6-1 Kasuga-Park, Kasuga, Fukuoka 816-8580, Japan
E-mail: michibata@riam.kyushu-u.ac.jp

August 26, 2020

Dear Prof. Corinna Hoose,

Thank you very much for your efforts in handling this manuscript. Enclosed please find our revised manuscript (acp-2020-232) submitted to *Atmospheric Chemistry and Physics*. It has been revised according to the referees' comments as shown in our response letters also attached.
We wish this manuscript deserves to publication.

Sincerely,

Takuro Michibata

# Response to Reviewer #1 of acp-2020-232

Dear Reviewer #1,

Thank you very much for taking your time to review our paper. We think that your comments greatly help improve the manuscript. We have revised the manuscript according to your comments as explained below with point-by-point responses to your comments. We hope that the revision is enough to address your comments to make the manuscript now acceptable for publication in *ACP*.

**[RC]: *Referee comment***
**[AC]: Author comment**

## Reviewer #1:
## General comments:

**[RC]** *This manuscript demonstrates the impact of falling hydrometeors on the effective radiative forcing of aerosol-cloud interactions in MIROC6 by modifying their microphysics from diagnostic precipitation to prognostic precipitation. The authors find that the large deviation in ERF(aci) in the old scheme is significantly improved as the magnitude of ERF(aci) is reduced. A series of sensitivity tests reveal that prognostic snow has substantial impact on both shortwave and longwave forcing induced by aerosols. This is an excellent modeling work, particularly that the impacts of many physical processes relating to aerosol-cloud interactions are quantified, as illustrated in Figure 4. However, there are some issues need to be clarified before accepted for publication.*

**[AC]** We would like to thank referee #1 for his/her positive comments and suggestions. We agree with the referee's comment that the manuscript needs more discussion about the physical mechanisms behind the snow-induced buffering ACI. We have added a more detailed description of the structural difference between DIAG and PROG, the roles of aerosol scavenging processes, and limitation of the present study, as shown in **[AC1]**, **[AC2]**, **[AC3]**, **[AC4]**, **[AC5]**, and **[AC16]** below.
In the revised manuscript, we have improved the method for estimating ERFaci in MIROC through providing "clean-sky ERFaci" based on Ghan (2013) to preclude contamination by aerosol-radiation interaction in cloudy-sky condition, according to the other referee's comment (Figures R2–R4; **[AC6]**). Furthermore, we have added a new estimate of multi-satellite ERFaci which considers the retrieval error based on Ma et al. (2018), as shown in Figure R3.
The reply and corrections on individual comments are shown below.

## Major concerns:

**[RC1]** *ERF(aci) is determined not only by changes in optical properties of cloud and precipitating particles, but also by changes in the cloud cover, particularly in GCM. In the text, the authors only show that the simulated cloud cover is "in good agreement" with the observation (although I think underestimation of high clouds is quite severe). However, the aerosol-induced change in cloud cover is not discussed at all.*

**[AC1]** Thank you for your important comment. This study does not discuss the contribution of changes in cloud cover to ERFaci, but it can also contribute to ERFaci although the magnitude might be relatively minor compared to the CLWP adjustment (e.g., Mülmenstädt et al., 2019; Gryspeerdt et al., 2020). The ERFaci correlates the PD minus PI change in CLWP robustly than that in cloud cover (Gettelman, 2015) as shown in Figure R1 because aerosol effects are directly linked to CLWP rather than cloud fraction by modifying the mass conversion rate from cloud water to rainwater that itself relates to the treatment of precipitation (i.e., DIAG vs PROG). However, there might be a feedback from precipitation treatment onto cloud fraction and thus it is nevertheless important in future studies to quantify the impact of precipitation modeling on relative contributions of the CLWP adjustment and cloud fraction adjustment through decomposing the forcing into the two components (Mülmenstädt et al., 2019). We have added brief arguments of this issue as follows (Section 5, Line 239): "This study primarily focused on ERFaci sensitivities to the CLWP adjustment rather than cloud fraction

adjustment, because aerosol effects are directly linked to the CLWP change through the modification of the mass conversion rate from cloud water to rainwater that itself relates to the treatment of precipitation (i.e., DIAG vs PROG). However, it is important in future studies to separating the ACI into the Twomey forcing and rapid adjustments of CLWP and cloud fraction (e.g., Goren and Rosenfeld, 2014; Mülmenstädt et al., 2019) for better understanding how the treatment of precipitation influences micro- and macroscopic cloud properties (Michibata and Suzuki, 2020), which relates to the fundamental inter-model spread in ERFaci (Gryspeerdt et al. 2020; Bellouin et al., 2020).".
We have also modified the description of the modeled cloud cover (Section 2.2) according to the comment.

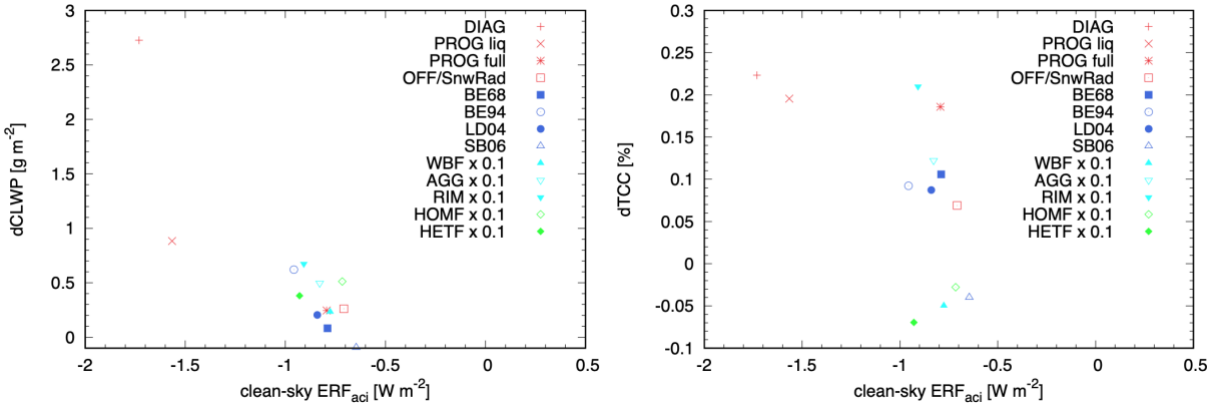


**Figure R1.** The relation between clean-sky ERFaci and **(left)** change in CLWP and **(right)** change in total cloud cover (TCC) from preindustrial to present-day conditions. Plots in red are tests of different precipitation framework, plots in blue are liquid autoconversion tests, plots in cyan are ice microphysics tests, and plots in green are tests for freezing processes.

**[RC2]** *From this manuscript, it is not clear to me how the aerosol scavenging process works in MIROC6 DIAG or PROG version. I suppose that PROG can simulate aerosol washout more realistic with falling rain and snow, and both ERF(aci) and ERF(ari) could be influenced.*
**[AC2]** According to our parallel analysis that was focused on sensitivities of ERFaci to the scavenging process, both wet-scavenging and coalescence scavenging are found to contribute to decreasing the magnitude of ERFaci. The enhancement of accretion and thus precipitation in the PROG simulation results in a more efficient scavenging process, which weakens the magnitude of the ACI (accretion-driven buffering mechanisms) as detailed in our recent publication (Michibata and Suzuki, 2020). We have added this argument as follows (Line 199): "Although the ERFaci variations with changing liquid and ice microphysical processes do not reach the difference of ERFaci between the DIAG and PROG (i.e., 54%), both wet-scavenging of aerosols and coalescence scavenging of cloud droplets also contribute to the ACI reduction (McCoy et al., 2020) due to the accretion-driven buffering mechanisms (Michibata and Suzuki, 2020), which should explain the remaining part of the ERFaci difference.".

**[RC3]** *This manuscript primarily focuses on the SW, while there is very little discussion about LW. The change in ERF(aci)-LW only attributes to "adjustment induced by snow together with its radiative effect" (Line 139). It is way too brief. The authors should elaborate the physical processes related to the "adjustment".*
**[AC3]** The following discussion has been added (Line 141): "The LW ERFaci is significant over the Indian Ocean and Southeast Asia (not shown), which is also similar to the other model, CAM5-MARC-ARG (Grandey et al., 2018). This is attributable to the increased ice nuclei (IN) due to biomass burning for example, partly supporting the convective invigoration (Rosenfeld et al., 2014) although GCMs do not have enough capability to resolve the convective cloud systems. The increased IN results in a faster glaciation and thus enhances snowfall due to the WBF process (i.e., glaciation

indirect effect). These mixed- and ice-phase microphysical processes are more elaborated in the PROG scheme, and the associated LW change induced by snow is incorporated only in the PROG, which contributes to the higher LW ERFaci across the globe.".

**[RC4]** *The authors claim that significant reduction in ERF(aci) well corresponds to snow water path (SWP) geographically (Fig. S3). It seems not true for me, particularly over the Southern Ocean. In contrast, the correlation between CLWP (Fig. S4) and ERF(aci) (Fig. 1) looks very high. It may imply that the change in ERF(aci) is primarily determined by CLWP change, and its relation with SWP is not so important.*
**[AC4]** The ERFaci primarily correlates with the change in CLWP through PI to PD as pointed by the reviewer. Since anthropogenic aerosols are very limited over the remote ocean, particularly over the Southern Ocean, the ERFaci is somewhat noisy and insignificant. What the authors are describing here is that the geographical difference of ERFaci between the DIAG and PROG is similar to the SWP distribution over East Asia, Europe, and North America where anthropogenic pollution dominates. The CLWP should increase with aerosols for both DIAG and PROG due to the cloud lifetime effect, but the significant part of increased cloud water contributes to the source of rain and snow (Fig. 3) when the model prognoses precipitating hydrometeors, and the latter plays a key role of the buffering of ACI (Fig. 4) over these anthropogenic regions.

**[RC5]** *The sequence of inference in Section 4 is complicated and not straightforward to me. The authors fist state that SWP susceptibility is correlated to LWP susceptibility (which I think a little weak) and propose a hypothesis that riming is important to reduce the optical depth of clouds. However, the sensitivity test clearly reveal the importance of riming (Fig. 4). That is, the sensitivity experiment should be considered as the basis of speculation, not the supporting evidence to the hypothesis.*
**[AC5]** The hypothesis that the snow-induced buffering of ACI is mainly due to the riming process is one of the interpretations based on sensitivity tests and previous studies (e.g., Lohmann, 2017) as pointed by the reviewer. Since the mixed-phase clouds are influenced by the larger number of microphysical processes than warm-phase clouds, constraining the physical mechanisms of the buffering may be still difficult due to the limitation of isolating feedbacks from multiple microphysical processes. This needs a theoretical approach and idealized process modeling (Glassmeier and Lohmann, 2016; Glassmeier et al., 2019) in addition to a GCM study, which are our important future work beyond the present study. In the revised manuscript, we have added these arguments about the relevant works to solidify the process-level understanding of snow-induced buffering hypothesis.
Section 5 (Line 238): "Furthermore, a theoretical approach (Glassmeier and Lohmann, 2016) and idealized process modeling (Glassmeier et al., 2019) are also required urgently to solidify the process-level understanding of snow-induced buffering hypothesis, which are our important future work beyond the present study."

## Minor points:

**[RC6]** *It seems to me that Figure 4 only consider the changes in ERF(aci)-SW because snow radiation is to increase ERF here. If it is the case, the figure caption and the description in the X-axis need to be more clear.*
**[AC6]** Figure 4 considers the net changes in ERFaci, but the sign of the "snow radiation" in the initial submission was wrong. This should be positive (+12.1%) because the inclusion of snow radiative effect enhances the magnitude of the ACI from -0.71 W $m^{-2}$ (PROG OFF/SnwRad) to -0.79 W $m^{-2}$ (PROG ON/SnwRad). The homogeneous freezing was also incorrect in sign, but the other items were all appropriate.
In the revised manuscript, the values of ERFaci are updated by considering the "clean-sky" condition based on Ghan (2013) as suggested by the other reviewer #2. Please be aware that Figures 1, 2, and 4 have been changed in this regard (see Figures R2–R4 below), but the conclusion of this paper does not change.

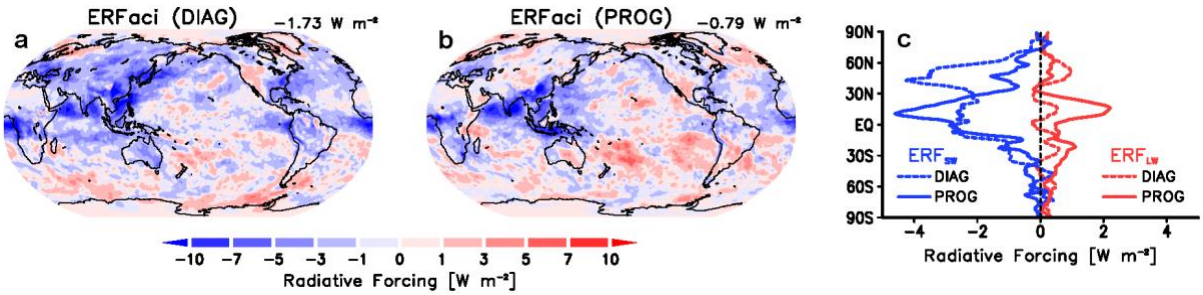


**Figure R2** (original Figure 1). Geographical distribution of the annual mean clean-sky ERFaci for the **(a)** DIAG and **(b)** PROG precipitation schemes. ERFaci is decomposed into (red) longwave and (blue) shortwave components in the **(c)** zonal mean field for the (dashed) DIAG and (solid) PROG schemes.

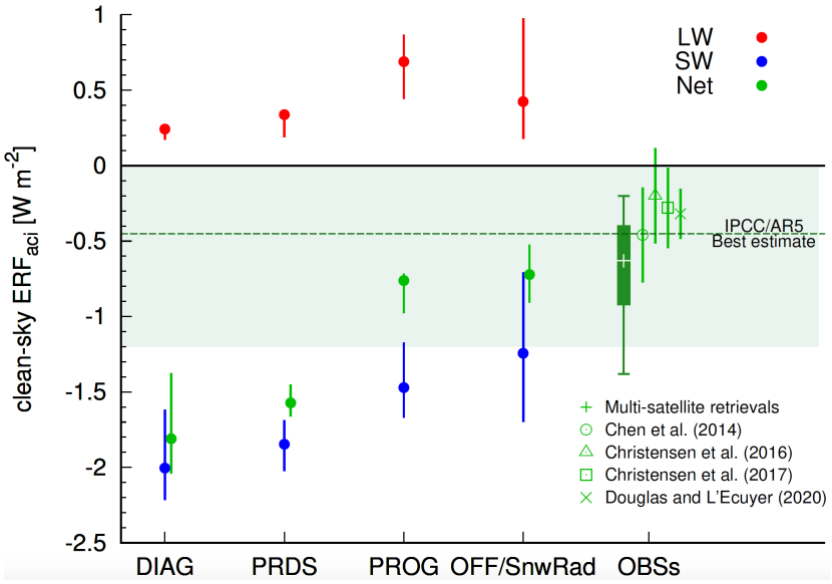


**Figure R3** (original Figure 2). ERFaci (Net ERFaci in green; LW ERFaci in red; SW ERFaci in blue) simulated from MIROC6 with different precipitation frameworks. The Net ERFaci values from observation-based studies (Chen et al., 2014; Christensen et al., 2016, 2017; Douglas and L'Ecuyer, 2020) and their probable range (box-whisker) calculated by correcting the effect of retrieval limitations (Michibata and Suzuki, 2020) based on Ma et al. (2018) are also shown. Error bars and plots in MIROC6 represent the minimum/maximum and median of the interannual variability, respectively. Shaded in light-green is the uncertainty range of ERFaci estimated from IPCC AR5 (Boucher et al., 2013). The prognostic rain with diagnostic snow scheme is denoted as "PRDS". The sensitivity experiment without snow radiative effects is denoted as "OFF/SnwRad".

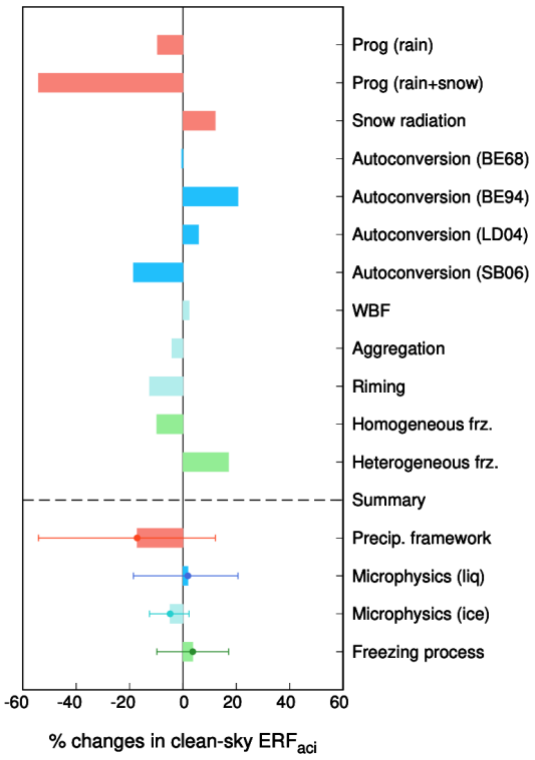


**Figure R4** (original Figure 4). Percentage change of global annual mean clean-sky ERFaci in response to (red) the precipitation treatment, (blue) liquid microphysics, (cyan) ice microphysics, and (green) nucleation of new ice particles due to freezing. Error bars represent the minimum and maximum range for each component considered in this study.

**[RC7]** *Line 87: What is the standard time step in MIROC6 as the sub-time step is 60 s?*
**[AC7]** The standard model timestep is 12 min in MIROC6 used in this study. We have added the information in the revised manuscript (Line 97).

**[RC8]** *Line 95: Does it mean PD and PI simulations use the same SST and sea ice?*
**[AC8]** Yes, PI simulations refer only to the aerosol emissions, and greenhouse gases and SSTs remain at the PD conditions. The differences represent only the aerosol emissions, and is the standard way for diagnosing aerosol ERFs.

**[RC9]** *Line 108: WBF should be spelled out.*
**[AC9]** We have defined the term here with relevant references (Wegener, 1911; Bergeron, 1935; Findeisen, 1938) in the revised manuscript.

**[RC10]** *Line 110: ". . . were returned. . . " Does it mean the simulations without TOA balance are not used in analysis?*
**[AC10]** Yes, all the experiments used in this study are satisfied with the imbalance of TOA radiation within 1.0 W m$^{-2}$. Model tuning was conducted by modifying scale factor for accretion rate but not autoconversion for warm rain process, because the latter can influence the magnitude of ACI due to the direct relation to droplet number (Michibata and Takemura, 2015; Jing et al., 2019) and thus the precipitation initiation (Mülmenstädt et al., 2020). This is effective for modifying SW radiation, but if needed, cloud ice and snow processes were also tuned for modifying LW radiation by changing scale factors for the fall speed of hydrometeors, which may be uninfluential on ERFaci because they are not involved in the hydrometeor number densities. These tuning strategies have been added in the revised manuscript according to the comments also by the other reviewer.

**[RC11]** *Line 123: This argument regarding ERF(ari) and ERF(aci) is quite indirect. Why not just show the values of these two terms?*
**[AC11]** Since the ARI and ACI are related to each other, it is difficult to separate into ERFari and ERFaci. We have modified the value of ERFaci throughout the manuscript by replacing clean-sky ERFaci as shown in **[AC6]**.

**[RC12]** *Line 126: "i.e., close to zero" Its meaning is ambiguous.*
**[AC12]** This has been removed, thanks.

**[RC13]** *Line 144: "only the latter process. . ." Should be "former"?*
**[AC13]** No, this sentence is correct. The autoconversion process depends on $N_c$ but the accretion process does not.

**[RC14]** *Figure 3: the description in X-axis should be CLWP instead of LWP.*
**[AC14]** We have modified the X-label and caption of Figure 3 as shown below (Figure R5).

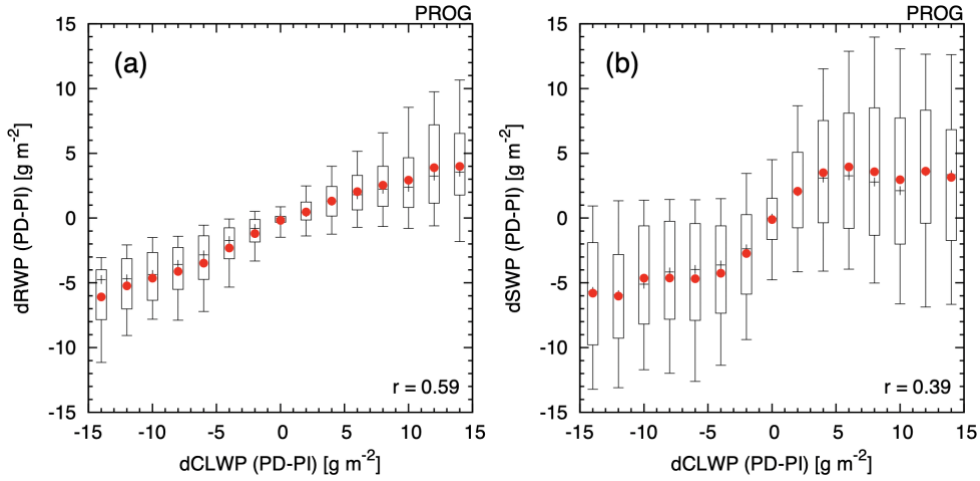


**Figure R5** (original Figure 3). Relationship between the change in annual mean CLWP and that in annual mean **(a)** RWP and **(b)** SWP, from the change in aerosols from PI to PD conditions, simulated using the PROG scheme. Box-whisker plots represent the 10th, 25th, 50th (black "+"), 75th, and 90th percentiles of the data within each bin based on the annual mean. Plots in red show the mean. The correlation coefficient ($r$) is given in the figure.

**[RC15]** *Line 174: "water mass suspended in the atmosphere" Does it mean cloud only?*
**[AC15]** Yes, this means cloud water. We have modified this sentence.

**[RC16]** *Line 175: If the total mass is the same, this argument holds. However, in this simulation, the total mass in PROG is larger than DIAG, and then the optical thickness of cloud+precipitation in PROG can be larger than that of cloud only in DIAG.*
**[AC16]** Thank you for the important comment. The total mass of cloud and precipitation hydrometeors is somewhat different between the DIAG and PROG as pointed by the reviewer and our previous study (Michibata et al., 2019). However, this does not primarily determine the ERFaci, and the magnitude of the ERFaci is determined by the changes of cloud and precipitation hydrometeors through PI to PD. If models prognose precipitating hydrometeors as well, the PD-PI change of clouds is shared with precipitating hydrometeors which are less sensitive to SW radiation, which weakens the cooling SW effect significantly. This mechanism can therefore be robust even if the total mass is not the same between the DIAG and PROG.

## References:


Bergeron, T. (1935). On the physics of cloud and precipitation. Proces verbaux de l'association de meteorologie, intl. union of geod. and geophys., paris (pp. 156–178).

Bellouin, N., Quaas, J., Gryspeerdt, E., Kinne, S., Stier, P.,Watson-Parris, D., et al. (2020). Bounding global aerosol radiative forcing of climate change. Reviews of Geophysics, 58, e2019RG000660. https://doi.org/10.1029/2019RG000660

Douglas, A., and L'Ecuyer, T. (2020). Quantifying cloud adjustments and the radiative forcing due to aerosol-cloud interactions in satellite observations of warm marine clouds. Atmospheric Chemistry and Physics, 20, 6225–6241.

Findeisen, Z. (1938). Kolloid meteorologische vorgange bei neiderschlags-bildung. Meteorologische Zeitschrift, 55, 121–133

Gettelman, A. (2015). Putting the clouds back in aerosol–cloud interactions. Atmospheric Chemistry and Physics, 15, 12,397–12,411. https:// doi.org/10.5194/acp-15-12397-2015

Ghan, S. J. (2013). Technical note: Estimating aerosol effects on cloud radiative forcing. Atmospheric Chemistry and Physics, 13, 9971–9974. doi:10.5194/acp-13-9971-2013

Glassmeier, F., and U. Lohmann (2016), Constraining precipitation susceptibility of warm, ice- and mixed-phase clouds with microphysical equations, Journal of the Atmospheric Science, 73, 5003–5023, doi:10.1175/JAS-D-16-0008.1.

Glassmeier, F., Hoffmann, F., Johnson, J. S., Yamaguchi, T., Carslaw, K. S., and Feingold, G. (2019). An emulator approach to stratocumulus susceptibility, Atmos. Chem. Phys., 19, 10191–10203, https://doi.org/10.5194/acp-19-10191-2019.

Goren, T., and Rosenfeld, D. (2014). Decomposing aerosol cloud radiative effects into cloud cover, liquid water path and Twomey components in marine stratocumulus, Atmospheric Research, 138, 378–393.

Grandey B. S., et al. (2018). Effective radiative forcing in the aerosol–climate model CAM5.3-MARC-ARG, Atmospheric Chemistry and Physics, 18, 15783–15810

Gryspeerdt, E., Mülmenstädt, J., Gettelman, A., Malavelle, F. F., Morrison, H., Neubauer, D., et al. (2020). Surprising similarities in model and observational aerosol radiative forcing estimates. Atmospheric Chemistry and Physics, 20, 613–623. https://doi.org/10.5194/ acp-20-613-2020

Jing, X., Suzuki, K., and Michibata, T. (2019). The key role of warm rain parameterization in determining the aerosol indirect effect in a global climate model. Journal of Climate, 32, 4409–4430.

Mülmenstädt, J., et al. (2020). Reducing the aerosol forcing uncertainty using observational constraints on warm rain processes, Science Advances, 6, eaaz6433.

Mülmenstädt, J., Gryspeerdt, E., Salzmann, M., Ma, P.-L., Dipu, S., and Quaas, J. (2019). Separating radiative forcing by aerosol–cloud interactions and fast cloud adjustments in the ECHAM-HAMMOZ aerosol-climate model using the method of partial radiative perturbations. Atmospheric Chemistry and Physics, 19, 15,415–15,429. https://doi.org/10.5194/acp-19-15415

Ma, P. L., Rasch, P. J., Chepfer, H., Winker, D. M., and Ghan, S. J. (2018). Observational constraint on cloud susceptibility weakened by aerosol retrieval limitations. Nature Communications, 9, 2640. doi:10.1038/s41467-018-05028-4

McCoy, D., Field, P., Gordon, H., Elsaesser, G., and Grosvenor, D. (2020). Untangling causality in midlatitude aerosol-cloud adjustments. Atmospheric Chemistry and Physics, 20, 4085–4103. https://doi.org/10.5194/acp-20-4085-2020

Michibata, T., and Suzuki, K. (2020). Reconciling compensating errors between precipitation constraints and the energy budget in a climate model. Geophysical Research Letters, 47, e2020GL088340. https://doi.org/ 10.1029/2020GL088340

Michibata, T., and Takemura, T. (2015). Evaluation of autoconversion schemes in a single model framework with satellite observations. Journal of Geophysical Research: Atmospheres, 120, 9570–9590.

Wegener, A., 1911: Thermodynamik der Atmosphäre. J. A. Barth, 331 pp.


Thank you very much again for reviewing our paper.

Sincerely yours,

Takuro Michibata

# Response to Reviewer #2 of acp-2020-232

Dear Reviewer #2 (Johannes Mülmenstädt),

Thank you very much for taking your time to review our paper. We think that your comments greatly help improve the manuscript. We have revised the manuscript according to your comments as explained below with point-by-point responses to your comments. We hope that the revision is enough to address your comments to make the manuscript now acceptable for publication in *ACP*.

**[RC]: *Referee comment***
**[AC]: Author comment**

## Reviewer #2 (Johannes Mülmenstädt):

**[RC]** *I have reviewed "Snow-induced buffering in aerosol–cloud interactions" by Takuro Michibata et al. The authors present an interesting set of sensitivity studies that show that prognostic snowfall in their GCM strongly reduces ERFaci compared to diagnostic snowfall, in large part because the longer residence time of snow leads to greater collection of cloud water by snow, which reduces the relative importance of warm phase ACI. Based on my own work, I think this is a plausible mechanism. There are a few potential weak links in the argument, which I will point out below. I don't think those should hold up publication of this potentially very useful result; after all, no paper is ever the final word on any topic. I recommend minor revisions to clarify the points I list below.*
**[AC]** We would like to thank Johannes Mülmenstädt for his carefully reading our manuscript and for giving insightful comments. We have revised the manuscript according to the referee comments.
In the revised manuscript, we have added a new estimate of multi-satellite ERFaci which considers the retrieval error based on Ma et al. (2018), as shown in Figure R3 (see **[AC3]** below). Furthermore, we have improved the method for estimating ERFaci in MIROC through providing "clean-sky ERFaci" based on Ghan (2013) to preclude contamination by aerosol-radiation interaction in cloudy-sky condition (see **[AC4]** for details).
The reply and corrections on individual comments are shown below.

### Major points

**[RC1]** *l. 110: The tuning strategy needs to be described in more detail. The worry with retuning is that the ERFaci difference may not be due to the change that was intentionally made, but due to the retuning.*
**[AC1]** Thank you for sharing your recent study which documents the link between tuning processes and ERFaci as commented in **[RC7]**. In our study, we primarily tuned the warm rain efficiency by modifying scale factor for accretion rate but not autoconversion because the latter can influence the magnitude of ACI due to the direct relation to droplet number (Michibata and Takemura, 2015; Jing et al., 2019) and thus the precipitation initiation (Mülmenstädt et al., 2020). This is effective for modifying SW radiation, but if needed, cloud ice and snow processes were also tuned for modifying LW radiation by changing scale factors for the fall speed of hydrometeors, which may be uninfluential on ERFaci because they are not involved directly in the hydrometeor number densities. We have added these statements in this paragraph.

**[RC2]** *l. 170 ff.: This is a question rather than a comment. From the conclusion of the paper, I would have expected the relationship between dLWP and dSWP to be the opposite – that when there is more snow, it would lead to more efficient removal of liquid cloud water. Would you mind making these plots separately for supercooled and nonsupercooled water?*

**[AC2]** This is a very important point. Considering the instantaneous response, the more snow should result in more efficient removal of the underlying cloud water due to collection processes, as the reviewer pointed. However, this does not always mean that the relationship between dCLWP and dSWP should be negative because the increased CLWP with aerosols (dCLWP > 0) contributes to additional sources of rain and snow (dRWP > 0; dSWP > 0), which would make the positive relationship in the monthly mean scale. Although the increased response of CLWP with aerosols through PI to PD is basically the same for both DIAG and PROG due to the cloud lifetime effect, the precipitation-driven collection of cloud droplets in PROG buffers the dCLWP (not mean negative) and thus the magnitude of ACI. The significant buffering of ACI can be seen when the model prognoses snow (Fig. 4) particularly over anthropogenic regions where snow is abundant, which does not conflict the positive relationship between dCLWP and dSWP.
To understand how the dCLWP-dSWP relation depends on the cloud regime, we further looked at the plot for supercooled and nonsupercooled regimes separately (Figure R6). The relationship between dCLWP and dSWP is more robust in the supercooled regime than in the nonsupercooled regime, implying that the mixed-phase cloud microphysics is a key driver to the snow-induced ACI buffering. Although we did not obtain a negative correlation between dCLWP and dSWP from this analysis, a theoretical approach and idealized process modeling should be required for future study to solidify the process-level understanding of snow-induced buffering hypothesis.
We have added the following sentence in the revised manuscript (Line 238): "Furthermore, a theoretical approach (Glassmeier and Lohmann, 2016) and idealized process modeling (Glassmeier et al., 2019) are also required urgently to solidify the process-level understanding of snow-induced buffering hypothesis, which are our important future work beyond the present study."

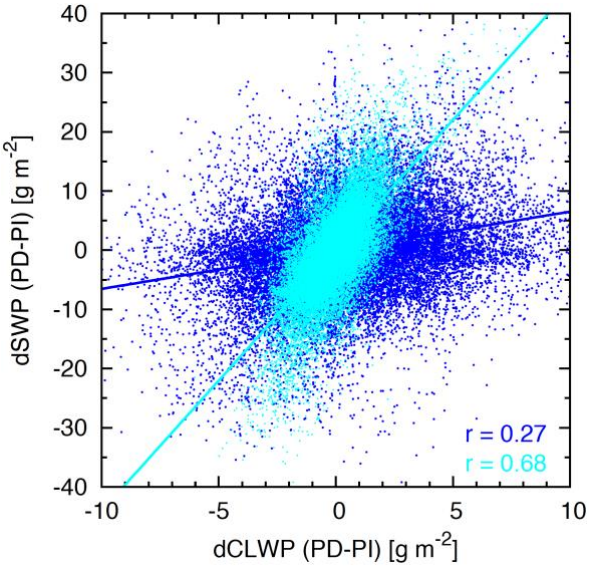


**Figure R6**. Relationship between the change in annual mean CLWP (nonsupercooled in blue and supercooled in cyan) and that in annual mean SWP, from the change in aerosols from PI to PD conditions, simulated using the PROG scheme. The correlation coefficients (*r*) are given in the figure.

## Minor points

**[RC3]** *l. 39 ff.: I don't think this argument is logically consistent. First, the authors say ERFaci in GCMs is "too negative" compared to satellite studies (I would prefer "more negative", since satellite studies have their own problems). But then they cite a (problematic) satellite study with a very negative SW ERFaci to argue that the problem is with the models' LW ERFaci. The rest of the paragraph is fine, but I would suggest removing the first two sentences.*

**[AC3]** Yes, satellite retrievals also include uncertainties which may underestimate ERFaci because satellites undersample the weak-aerosol regime, where the cloud sensitivity to aerosol is largest (Ma et al., 2018). In the revised manuscript, we have added multi-satellite ERFaci which considers the retrieval errors based on Ma et al. (2018) as shown in Michibata and Suzuki (2020), but the DIAG scheme still shows more negative ERFaci (Figure R3). This implies that there might be unknown compensating aerosol warming effects that are missing in current GCMs, possibly through mixed-phase clouds (Lohmann and Hoose, 2009).
We therefore have remained the sentences but modified slightly as follows (Lines 39-42): "As a consequence of the challenges described above, GCMs tend to show more negative ERFaci than that inferred from satellite retrievals (Quaas et al., 2009; Chen et al., 2014) even though retrieval errors (Ma et al., 2018) are considered (Michibata and Suzuki, 2020). This suggests that current GCMs may be missing a compensating warming effect caused by aerosols.".

**[RC4]** *l. 111: Didn't Ghan (2013) show that the change in cloud radiative effect is not a good estimate of ERFaci because it contains pieces of ERFaci and ERFari?*
**[AC4]** In the revised manuscript, we have improved the method for estimating ERFaci in MIROC through providing "clean-sky ERFaci" based on Ghan (2013) to preclude contamination by aerosol-radiation interaction in cloudy-sky condition. This revision changes Figures 1, 2, and 4. We have also added a new estimate of multi-satellite ERFaci which considers the retrieval error based on Ma et al. (2018), as presented in Michibata and Suzuki (2020) (please see also **[AC3]** above).

**[RC5]** *l. 130: It might be worth pointing out that the Heyn et al. (2017) behavior is present in the zonal mean distribution (wherever SW ERFaci becomes stronger [weaker], LW ERFaci also becomes stronger [weaker]), but not in the global mean.*
**[AC5]** The following sentence has been added in this paragraph (Line 128): "The zonal distribution shows that stronger (weaker) LW ERFaci accompanies stronger (weaker) SW ERFaci, which is in line with Heyn et al. (2017).".

**[RC6]** *Fig. 3: The legend should say what the aggregation is, i.e., are the box and whiskers calculated based on monthly mean grid boxes? Also, in my mind, "susceptibility" implies susceptibility to a measure of aerosol; I would call the LWP, RWP, and SWP changes dLWP etc.*
**[AC6]** The following explanation has been added in the caption: "Box-whisker plots represent the 10th, 25th, 50th (black "+"), 75th, and 90th percentiles of the data within each bin based on the annual mean.". The figure legend uses dCLWP, dRWP, and dSWP, instead of "susceptibility".

**[RC7]** *l. 190: See my comment about retuning above. For example, in Mülmenstädt et. al. (2020), https://doi.org/10.1126/sciadv.aaz6433, we found that ERFaci is fairly insensitive to the cloud droplet number exponent but very sensitive to the liquid water mixing ratio exponent and the overall normalization in the Khairoutdinov and Kogan (2000) autoconversion scheme. If the retuning strategy for the change in Nc exponent involves changing other parts of the autoconversion, that may result in an overly strong apparent ERFaci change. Of course, which parameters ERFaci is sensitive will vary between models.*
**[AC7]** Thank you for your very important comment. We have added a more detailed description of the tuning (Section 2.2) as answered in **[AC1]**. We have also modified the sentence citing the suggested work.

**[RC8]** *l. 210: Is this list complete? E3SM has prognostic snow (Rasch et al., 2019), and I believe GISS Model E3 does too. HadGEM3 may do so as well.*
**[AC8]** Thank you for the information. The authors have contacted several modeling centers to know the latest model spec on the treatment of precipitation. Some replies suggested that now more GCMs include two-moment prognostic precipitation with snow radiative effect (e.g., E3SM, GISS-Model E3). In the revised paper (Lines 210 and 230), this sentence has been slightly changed citing a relevant paper (Li et al., 2020) which overviews the latest model status in CMIP6.

## References:


Chen, Y.-C., Christensen, M. W., Stephens, G. L., and Seinfeld, J. H. (2014). Satellite-based estimate of global aerosol-cloud radiative forcing by marine warm clouds. Nature Geoscience, 7, 643–646.

Ghan, S. J. (2013). Technical note: Estimating aerosol effects on cloud radiative forcing. Atmospheric Chemistry and Physics, 13, 9971–9974. doi:10.5194/acp-13-9971-2013

Glassmeier, F., and U. Lohmann (2016), Constraining precipitation susceptibility of warm, ice- and mixed-phase clouds with microphysical equations, Journal of the Atmospheric Science, 73, 5003–5023, doi:10.1175/JAS-D-16-0008.1.

Glassmeier, F., Hoffmann, F., Johnson, J. S., Yamaguchi, T., Carslaw, K. S., and Feingold, G. (2019). An emulator approach to stratocumulus susceptibility, Atmos. Chem. Phys., 19, 10191–10203, https://doi.org/10.5194/acp-19-10191-2019.

Heyn I, Block K, Mulmenstadt J, Gryspeerdt E, Kuhne P, Salzmann M, Quaas J. Is the IPCC AR5 estimate of the aerosol effective radiative forcing too weak? (2017). Geophys Res Lett.

Jing, X., Suzuki, K., and Michibata, T. (2019). The key role of warm rain parameterization in determining the aerosol indirect effect in a global climate model. Journal of Climate, 32, 4409–4430.

Li, J. L. Frank et al. (2020). An Overview of CMIP5 and CMIP6 Simulated Cloud Ice, Radiation Fields, Surface Wind Stress, Sea Surface Temperatures, and Precipitation Over Tropical and Subtropical Oceans. Journal of Geophysical Research, 125, e2020JD032848

Lohmann, U. and Hoose, C. (2009). Sensitivity studies of different aerosol indirect effects in mixed-phase clouds, Atmospheric Chemistry and Physics, 9, 8917–8934.

Mülmenstädt, J., et al. (2020). Reducing the aerosol forcing uncertainty using observational constraints on warm rain processes, Science Advances, 6, eaaz6433.

Ma, P. L., Rasch, P. J., Chepfer, H., Winker, D. M., and Ghan, S. J. (2018). Observational constraint on cloud susceptibility weakened by aerosol retrieval limitations. Nature Communications, 9, 2640. doi:10.1038/s41467-018-05028-4

Michibata, T., and Suzuki, K. (2020). Reconciling compensating errors between precipitation constraints and the energy budget in a climate model. Geophysical Research Letters, 47, e2020GL088340. https://doi.org/ 10.1029/2020GL088340

Quaas, J., Ming, Y., Menon, S., Takemura, T., Wang, M., Penner, J. E., et al. (2009). Aerosol indirect effects general circulation model intercomparison and evaluation with satellite data. Atmospheric Chemistry and Physics, 9, 8697–8717. https://doi.org/10.5194/ acp-9-8697-2009

Rasch, P. J., Xie, S., Ma, P.-L., Lin, W., Wang, H., Tang, Q., et al. (2019). An overview of the atmospheric component of the Energy Exascale Earth System Model. Journal of Advances in Modeling Earth Systems, 11(8), 2377–2411. https://doi.org/10.1029/2019MS001629


Thank you very much again for reviewing our paper.

Sincerely yours,

Takuro Michibata

# Snow-induced buffering in aerosol–cloud interactions

Takuro Michibata[1], Kentaroh Suzuki[2], and Toshihiko Takemura[1]

[1]Research Institute for Applied Mechanics, Kyushu University, Fukuoka 816-8580, Japan
[2]Atmosphere and Ocean Research Institute, The University of Tokyo, Chiba 277-8568, Japan

**Correspondence:** Takuro Michibata (michibata@riam.kyushu-u.ac.jp)

**Abstract.** Complex aerosol–cloud–precipitation interactions lead to large differences in estimates of aerosol impacts on climate among general circulation models (GCMs) and satellite retrievals. Typically, precipitating hydrometeors are treated diagnostically in most GCMs, and their radiative effects are ignored. Here, we quantify how the treatment of precipitation influences the simulated effective radiative forcing due to aerosol–cloud interactions ($\mathrm{ERF_{aci}}$) using a state-of-the-art GCM with a two-moment prognostic precipitation scheme that incorporates the radiative effect of precipitating particles, and investigate how microphysical process representations are related to macroscopic climate effects. Prognostic precipitation substantially weakens the magnitude of $\mathrm{ERF_{aci}}$ (by approximately ~~75%~~54%) compared with the traditional diagnostic scheme, and this is the result of the increased longwave (warming) and weakened shortwave (cooling) components of $\mathrm{ERF_{aci}}$. The former is attributed to additional adjustment processes induced by falling snow, and the latter stems largely from riming of snow by collection of cloud droplets. The significant reduction in $\mathrm{ERF_{aci}}$ does not occur without prognostic snow, which contributes mainly by buffering the cloud response to aerosol perturbations through depleting cloud water via collection. Prognostic precipitation also alters the regional pattern of $\mathrm{ERF_{aci}}$, particularly over northern mid-latitudes where snow is abundant. The treatment of precipitation is thus a highly influential controlling factor of $\mathrm{ERF_{aci}}$, contributing more than other uncertain "tunable" processes related to aerosol–cloud–precipitation interactions. This change in $\mathrm{ERF_{aci}}$ caused by the treatment of precipitation is large enough to explain the existing difference in $\mathrm{ERF_{aci}}$ between GCMs and observations.

## 1 Introduction

Aerosols play significant roles in the climate system (Twomey, 1977; Albrecht, 1989) by modifying the radiation budget (aerosol–radiation interactions; ARI) and the hydrological cycle through interactions with clouds (aerosol–cloud interactions; ACI). Quantitative estimates of anthropogenic aerosol forcing, however, are still largely uncertain (Boucher et al., 2013) because of the complex interactions among aerosols, clouds, and climate across wide spatiotemporal scales (Mülmenstädt and Feingold, 2018). Reducing these uncertainties associated with the effect of aerosol forcing on climate is one of the most challenging issues in climate science (Seinfeld et al., 2016).

A key uncertainty arises from the complex response of clouds to aerosol perturbations (Wang et al., 2012). Clouds are considered to respond to perturbed aerosols in two opposing ways; i.e., the so-called "cloud lifetime" effect (Albrecht, 1989) and the "buffered system" effect (Stevens and Feingold, 2009), in a regime-dependent manner (Wood, 2012; Michibata et al., 2016). The cloud water susceptibility to aerosols depends strongly upon cloud type (Christensen et al., 2016), as well as

ambient environmental conditions (Toll et al., 2019), which results in non-monotonic cloud responses (Gryspeerdt et al., 2019) and therefore diverse impacts on climate (Chen et al., 2014).

These observational findings are also supported by process modeling studies using large-eddy simulations (Lebo and Feingold, 2014; Seifert et al., 2015). General circulation models (GCMs), however, show a large spread in cloud susceptibility to aerosols (Ghan et al., 2016; Zhang et al., 2016), and tend to overestimate the magnitude of ACI compared with satellite retrievals (Malavelle et al., 2017). This means that current GCMs are not able to reproduce the buffering of cloud responses to aerosol perturbations (Jing et al., 2019). Aerosol-induced radiative forcing at the top of the atmosphere (TOA) that includes rapid adjustments caused by ACI, termed effective radiative forcing ($\mathrm{ERF_{aci}}$), varies widely among GCMs (Shindell et al., 2013; Zelinka et al., 2014). This results in a "best estimate" of global annual mean $\mathrm{ERF_{aci}}$ of $-0.45\ \mathrm{W\,m^{-2}}$ with a 90% confidence interval of $-1.2$ to $0.0\ \mathrm{W\,m^{-2}}$ (Boucher et al., 2013), as reported in the fifth assessment report of the Intergovernmental Panel on Climate Change (IPCC AR5). This uncertainty range has remained large (e.g., Bellouin et al., 2020) since the early IPCC reports.

As a consequence of the challenges described above, GCMs tend to show ~~a stronger (i.e., too negative)~~ more negative $\mathrm{ERF_{aci}}$ than that inferred from satellite retrievals (Quaas et al., 2009; Chen et al., 2014) even though retrieval errors (Ma et al., 2018) are considered (Michibata and Suzuki, 2020). ~~Given that aerosols can exert a substantial cooling effect for fixed meteorology in shallow warm clouds (Rosenfeld et al., 2019),~~ This suggests that current GCMs may be missing a compensating warming effect caused by aerosols. The "missing warming" in GCMs may be solved by taking aerosol effects on (i) deep convective clouds (Wang et al., 2011) and (ii) mixed-phase clouds (Lohmann and Hoose, 2009) into consideration, as these effects can modify the ice microphysics due to aerosols and also lead to an adjustment in the longwave component (Lohmann, 2017). A recent multi-model analysis (Heyn et al., 2017) demonstrated that simpler GCMs that parameterize the aerosol effect on liquid-phase clouds alone have negligibly small longwave ERF, whereas more sophisticated GCMs that include microphysical adjustments of ice- and mixed-phase clouds as well as liquid-phase clouds produce larger magnitude ERF values for both the terrestrial ($\mathrm{ERF^{LW}}$) and solar ($\mathrm{ERF^{SW}}$) components. The changes to $\mathrm{ERF^{LW}}$ and $\mathrm{ERF^{SW}}$ were found to nearly cancel each other out and result in a net ERF ($\mathrm{ERF^{Net}}$) of a magnitude that is similar to that generated by the simpler GCMs. The robustness of this near cancelation, however, largely depends on how microphysical processes in ice- and mixed-phase clouds, which are typically much more complex than in liquid-phase clouds (Lohmann, 2017), are represented in GCMs.

Among these processes, precipitation processes involving falling hydrometeors (i.e., rain and snow) are particularly simplified in current GCMs, which is likely to lead to nonnegligible uncertainty in $\mathrm{ERF_{aci}}$ (Gettelman, 2015). In general, precipitation is treated diagnostically in GCMs (hereinafter "DIAG"), with precipitation being immediately removed from the atmosphere within a single model timestep. This overweights autoconversion relative to accretion to produce precipitation (Posselt and Lohmann, 2008), which results in the pronounced sensitivity of cloud water to aerosols because autoconversion is the only process that directly depends on aerosols (Gettelman et al., 2013). Snow also has significant effects on collection processes among other hydrometeors (Sant et al., 2015), as well as on atmospheric circulation (Li et al., 2014). However, snow-induced impacts on $\mathrm{ERF_{aci}}$ are much less understood (Waliser et al., 2011) because extremely limited GCMs incorporate prognostic precipitation with the radiative effects of falling hydrometeors (see discussion in Michibata et al. (2019)).

This study investigates this unexplored area of ACI, with a particular focus on precipitation (rain and snow) processes and their impacts on $\mathrm{ERF_{aci}}$, and with the goal of advancing our understanding of the fundamental linkage of microphysical process representations to their macroscopic climate effects. For this purpose, we use a recently developed global aerosol–climate model, MIROC6-SPRINTARS (Tatebe et al., 2019), which is implemented with a two-moment prognostic precipitation scheme (hereinafter "PROG") that includes the radiative effects of precipitation (Michibata et al., 2019). Through a comparison with the traditional DIAG scheme, we use the PROG-scheme model to identify the source of discrepancies in $\mathrm{ERF_{aci}}$ between GCMs and satellite observations that are related to precipitation processes. A suite of sensitivity experiments is also performed with the model to isolate the relative contributions of different microphysical processes to $\mathrm{ERF_{aci}}$ and to quantify how uncertainties inherent in these processes translate to $\mathrm{ERF_{aci}}$ uncertainty. This single-model approach has the advantage of not being affected by varying physics representations, as in the case of multi-model analysis (cf. Materials and Methods).

## 2 Materials and methods

### 2.1 MIROC6-SPRINTARS aerosol–climate model

We used version 6 of the global aerosol–climate model, MIROC6-SPRINTARS (Tatebe et al., 2019) in this work. The aerosol module, SPRINTARS (Takemura et al., 2009), predicts the mass mixing ratios of the main aerosol species in the troposphere (black carbon, organic matter, sulfate, soil dust, and sea salt) and gas-phase precursors of sulfate (sulfur dioxide and dimethyl sulfide) and organic matter (terpene and isoprene). The cloud microphysics are based on the prognostic probability density function (PDF) scheme, which represents the subgrid-scale variability of temperature and total water content (Watanabe et al., 2009), and is coupled to an ice microphysics scheme (Wilson and Ballard, 1999). The model treats cloud water and ice using a two-moment representation, by prognosing both mass and number mixing ratios (Takemura et al., 2009). Cloud droplet nucleation is represented by a Köhler-theory-based parameterization (Abdul-Razzak and Ghan, 2000). Note that although the standard version of MIROC6-SPRINTARS uses Berry's autoconversion parameterization (Berry, 1968), results presented in this paper apply an alternative formulation based on Khairoutdinov and Kogan (2000), which is used in the PROG version (Michibata et al., 2019) for a robust comparison (described later). The default MIROC6-SPRINTARS model treats precipitation diagnostically, and its radiative effect is not considered.

We also used another version of the model that employs a prognostic precipitation framework (Michibata et al., 2019). This version prognoses mass and number mixing ratios for both rain and snow, as well as cloud liquid and ice condensates (full two-moment scheme). Microphysical processes are calculated iteratively by using sub-time steps (60 s), except for the sedimentation of precipitation, which can be shorter subject to the vertical CFL criteria. The PROG scheme considers the radiative effect of precipitating hydrometeors. The particle shapes of solid hydrometeors are prescribed by assuming hexagonal columns for cloud ice and dendrite crystals for snow bulk categories, which correspond to elements of a radiation table (Yang et al., 2013). For more details, please refer to the model description for the latest version of MIROC6 (Tatebe et al., 2019; Michibata et al., 2019).

### 2.2 Experimental setup

We performed sets of simulations with different aerosol emissions for the years 2000 (present-day; PD) and 1850 (pre-industrial; PI). All simulations used prescribed climatological sea surface temperature and sea ice. Simulations were integrated for 6 years, with the last 5 years being used in the subsequent analysis. The model resolution was T85L40 (ca. 1.4° resolution in longitude and latitude with 40 vertical levels), and the standard model timestep was 12 min. ~~We have confirmed that the~~ The modeled cloud cover and its horizontal distribution (Fig. S1) are in good agreement with CALIPSO-GOCCP satellite data (Chepfer et al., 2010) in PROG but underestimated in DIAG, which were evaluated using the COSP2 satellite simulator package (Swales et al., 2018) using an additional full one-year run under the PD conditions.

Additional sensitivity experiments were performed, by replacing the precipitation framework, changing the liquid autoconversion scheme, and masking ice microphysics and aerosol freezing processes (discussed later in Sect. 4). To quantify how the treatment of precipitation influences the simulated $\mathrm{ERF_{aci}}$, two experiments; i.e., one that incorporates a prognostic treatment of rain but not snow (PRDS), and another that applies the full prognostic version (PROG), were compared with the default simulation with diagnostic precipitation (DIAG). To evaluate the snow radiative effect, a pair of simulations with and without snow radiation were also carried out using the PROG framework. For liquid microphysics, four commonly used autoconversion schemes (BE68 (Berry, 1968); BE94 (Beheng, 1994); LD04 (Liu and Daum, 2004); and SB06 (Seifert and Beheng, 2006)) were compared with the default PROG simulation using the KK00 scheme (Khairoutdinov and Kogan, 2000). Results from the sensitivity experiments which were adjusted by a factor of 0.1 for the ~~WBF effect~~ Wegener–Bergeron–Findeisen (WBF) process (Wegener, 1911; Bergeron, 1935; Findeisen, 1938), aggregation, riming efficiency, and freezing ratios of homo- and heterogeneous nucleation, were subtracted from the default PROG result to quantify the impact of the targeted process. ~~If needed, these experiments were retuned so that the imbalance of the radiative flux at the TOA remained within 1.0 $\mathrm{W\,m^{-2}}$.~~ In this study, $\mathrm{ERF_{aci}}$ is defined as the change in net cloud radiative forcing at the TOA under clean-sky (Ghan, 2013) with fixed ocean conditions, but allows atmospheric processes including rapid adjustments in the response to aerosol changes, from PI to PD (Boucher et al., 2013).

If needed, these experiments were retuned so that the imbalance of the radiative flux at the TOA remained within 1.0 $\mathrm{W\,m^{-2}}$. Model tuning was conducted by modifying scale factor for accretion rate but not autoconversion for warm rain process because the latter can influence the magnitude of ACI due to the direct relation to droplet number (Michibata and Takemura, 2015; Jing et al., 2019) and thus the precipitation initiation (Mülmenstädt et al., 2020). This is effective for modifying SW radiation, but if needed, cloud ice and snow processes were also tuned for modifying LW radiation by changing scale factors for the fall speed of hydrometeors, which may be uninfluential on $\mathrm{ERF_{aci}}$ because they are not involved directly in the hydrometeor number densities.

## 3 Weakening of $\mathrm{ERF_{aci}}$ with prognostic precipitation

Figure 1 compares geographical distributions of $\mathrm{ERF_{aci}}$ simulated by the DIAG and PROG models. In DIAG, a strong negative $\mathrm{ERF_{aci}}$ is observed over East Asia, Europe, and North America where anthropogenic pollution dominates. This is attributed to

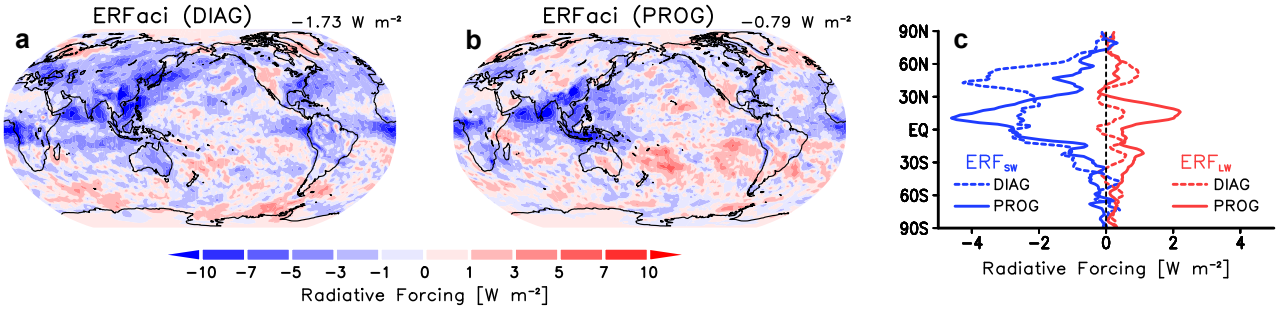


**Figure 1.** Geographical distribution of the annual mean clean-sky $\mathrm{ERF_{aci}}$ for the **(a)** DIAG and **(b)** PROG precipitation schemes. $\mathrm{ERF_{aci}}$ is decomposed into (red) longwave and (blue) shortwave components in the **(c)** zonal mean field for the (dashed) DIAG and (solid) PROG schemes.

the cloud lifetime effect caused by anthropogenic aerosols, which increases low warm clouds and hence shortwave reflectance. The global annual mean $\mathrm{ERF_{aci}}$ reaches ~~−1.1~~ −1.7 $\mathrm{W\,m^{-2}}$, which is ~~near the upper bound~~ outside the bound of the uncertainty range ($-1.2\ \mathrm{W\,m^{-2}}$) in IPCC AR5. The geographical pattern is consistent with other GCMs (Shindell et al., 2013; Zelinka et al., 2014).

In PROG, however, the majority of the strong negative forcing over anthropogenic regions is reduced significantly, resulting in a reduction of around ~~75%~~54% in global-mean $\mathrm{ERF_{aci}}$. Although the geographical pattern is somewhat different from previous reports using other GCMs (discussed in the next section), the global mean $\mathrm{ERF_{aci}}$ (~~−0.3~~ −0.8 $\mathrm{W\,m^{-2}}$) is much closer to satellite-based estimates (Chen et al., 2014; Christensen et al., 2016, 2017; Douglas and L'Ecuyer, 2020). ~~The total ERF associated with ARI and ACI ($\mathrm{ERF_{ari+aci}}$) in PROG ($-0.7\ \mathrm{W\,m^{-2}}$) is only half that generated by DIAG ($-1.4\ \mathrm{W\,m^{-2}}$), which means that the changes to $\mathrm{ERF_{ari+aci}}$ are driven mostly by ACI rather than ARI.~~ The total aerosol ERF associated with ARI and ACI ($\mathrm{ERF_{ari+aci}}$) in PROG ($-1.1\ \mathrm{W\,m^{-2}}$) is only half that generated by DIAG ($-2.1\ \mathrm{W\,m^{-2}}$).

This significant reduction ~~(i.e., closer to zero)~~ in $\mathrm{ERF_{aci}}$ in PROG results from a substantial weakening of $\mathrm{ERF_{aci}^{SW}}$ particularly over mid-latitudes of the Northern Hemisphere, and enhanced warming of $\mathrm{ERF_{aci}^{LW}}$ over low latitudes in both hemispheres (Fig. 1c). The zonal distribution shows that stronger (weaker) $\mathrm{ERF_{aci}^{LW}}$ accompanies stronger (weaker) $\mathrm{ERF_{aci}^{SW}}$, which is in line with Heyn et al. (2017). To understand the impact of precipitation treatment on $\mathrm{ERF_{aci}}$, decompositions of global mean $\mathrm{ERF_{aci}}$ into its SW and LW components are shown for alternate configurations of precipitation in MIROC6 (Fig. 2). Figure 2 confirms that the significant reduction of $\mathrm{ERF_{aci}}$ in PROG is contributed to by both increased $\mathrm{ERF_{aci}^{LW}}$ and weakened $\mathrm{ERF_{aci}^{SW}}$, in stark contrast to previous CMIP5 model results (Heyn et al., 2017) in which cloud-ice-induced changes to $\mathrm{ERF^{SW}}$ and $\mathrm{ERF^{LW}}$ cancel each other out to result in few net ERF changes within the DIAG framework. This difference in the present study from previous results is attributed to the snow-induced modulation of ACI newly incorporated into our model.

The impact of snow on ACI can be understood in more detail using the results shown in Fig. 2, which includes two intermediate versions of PROG; i.e., one that incorporates prognostic rain but diagnostic snow (PRDS) to isolate the relative impacts of rain vs snow on $\mathrm{ERF_{aci}}$, and one that represents prognostic rain and snow but without the radiative effects of snow

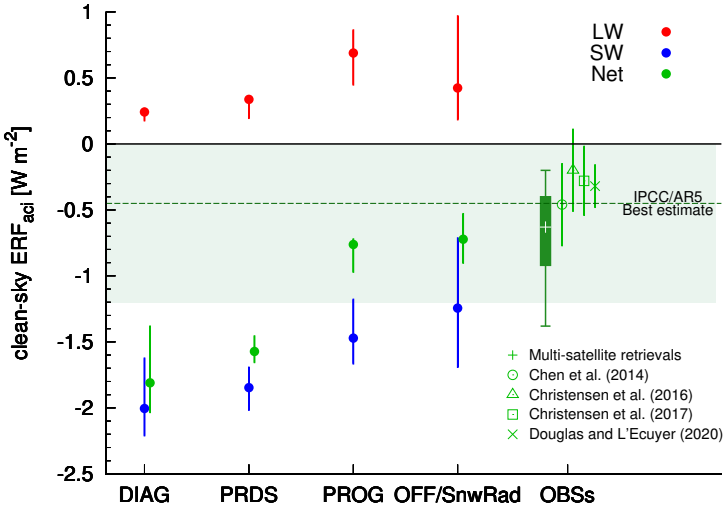


**Figure 2.** $\mathrm{ERF_{aci}}$ ($\mathrm{ERF_{aci}^{Net}}$ in green; $\mathrm{ERF_{aci}^{LW}}$ in red; $\mathrm{ERF_{aci}^{SW}}$ in blue) simulated from MIROC6 with different precipitation frameworks. The $\mathrm{ERF_{aci}^{Net}}$ values from observation-based studies (Chen et al., 2014; Christensen et al., 2016, 2017; ~~Ma et al., 2018~~; Douglas and L'Ecuyer, 2020) and their probable range (box-whisker) calculated by correcting the effect of retrieval limitations (Michibata and Suzuki, 2020) based on Ma et al. (2018) are also shown. Error bars and plots in MIROC6 represent the minimum/maximum and median of the interannual variability, respectively. Shaded in light-green is the uncertainty range of $\mathrm{ERF_{aci}}$ estimated from IPCC AR5 (Boucher et al., 2013). The prognostic rain with diagnostic snow scheme is denoted as "PRDS". The sensitivity experiment without snow radiative effects is denoted as "OFF/SnwRad".

(OFF/SnwRad). Regarding the LW component, the global mean $\mathrm{ERF_{aci}^{LW}}$ of PROG ($+0.7\ \mathrm{W\,m^{-2}}$) is more than twice as large as those of DIAG ($+0.2\ \mathrm{W\,m^{-2}}$) and PRDS ($+0.3\ \mathrm{W\,m^{-2}}$). The OFF/SnwRad simulation also shows weaker $\mathrm{ERF_{aci}^{LW}}$ relative to the standard PROG simulation (Fig. 2). These results suggest that the warming LW effect comes mainly from adjustments induced by snow together with its radiative effects, in addition to cloud-ice effects included in CMIP5 models as well as our model. The $\mathrm{ERF_{aci}^{LW}}$ is significant over the Indian Ocean and Southeast Asia (not shown), which is also similar to the other model, CAM5-MARC-ARG (Grandey et al., 2018). This is attributable to the increased ice nuclei (IN) due to biomass burning for example, partly supporting the convective invigoration (Rosenfeld et al., 2014) although GCMs do not have enough capability to resolve the convective cloud systems. The increased IN results in a faster glaciation and thus enhances snowfall due to the WBF process (i.e., glaciation indirect effect). These mixed- and ice-phase microphysical processes are more elaborated in the PROG scheme, and the associated LW change induced by snow is incorporated only in the PROG, which contributes to the higher $\mathrm{ERF_{aci}^{LW}}$ across the globe.

The PROG scheme also reduces the SW component ($\mathrm{ERF_{aci}^{SW}}$) relative to DIAG, particularly over anthropogenic regions (Fig. 1b) in the Northern Hemisphere mid-latitudes. A well-known mechanism for the reduction in $\mathrm{ERF_{aci}^{SW}}$ is the enhancement of accretion with a smaller contribution from autoconversion, as in PROG (not shown), with only the latter process depending upon the cloud droplet number concentration ($N_c$) (Posselt and Lohmann, 2008). The smaller contribution of autoconversion

in PROG mitigates the excessive cloud water susceptibility to aerosols that occurs in DIAG models (Gettelman et al., 2015; Michibata et al., 2019). However, Fig. 2 shows that the replacement in liquid-phase precipitation alone from DIAG to PRDS cannot explain the significant reduction of $\mathrm{ERF}_{\mathrm{aci}}^{\mathrm{SW}}$ from DIAG to PROG, suggesting that ice-phase processes involving falling snow influence the magnitude of $\mathrm{ERF}_{\mathrm{aci}}^{\mathrm{SW}}$, as discussed in the next section.

This reduction of $\mathrm{ERF}_{\mathrm{aci}}^{\mathrm{SW}}$ in PROG relative to DIAG is also impossible to explain by the response of cloud ice alone, because cloud ice should increase $\mathrm{ERF}_{\mathrm{aci}}^{\mathrm{SW}}$ towards more negative values because of aerosol-induced increases in cloud optical thickness. This is indeed what is happening with the DIAG framework in the CMIP5 multi-model results (Heyn et al., 2017), in which models with aerosol effects on cloud ice (not snow) show much stronger $\mathrm{ERF}_{\mathrm{aci}}^{\mathrm{SW}}$, which is large enough to cancel the enhancement of $\mathrm{ERF}_{\mathrm{aci}}^{\mathrm{LW}}$. In contrast, our PROG model reduces $\mathrm{ERF}_{\mathrm{aci}}^{\mathrm{SW}}$. We hypothesize that the prognostic treatment of snow plays an important role in weakening $\mathrm{ERF}_{\mathrm{aci}}^{\mathrm{SW}}$ through microphysical processes involving cloud water and snow, as discussed below.

## 4 Relationship of microphysics and $\mathrm{ERF}_{\mathrm{aci}}$

Next, we discuss the role of prognostic precipitation in determining $\mathrm{ERF}_{\mathrm{aci}}$ by addressing the following two questions raised in the previous section:

1. *Why does the geographical pattern of* $\mathrm{ERF}_{\mathrm{aci}}$ *in PROG differ from that of DIAG?*
2. *Why does the prognostic treatment of snow effectively weaken* $\mathrm{ERF}_{\mathrm{aci}}^{\mathrm{SW}}$*?*

To this end, we first explore how precipitating hydrometeors can modulate the cloud water susceptibility to perturbed aerosols. Figure 3 shows how the change in the cloud liquid water path (CLWP) relates to changes in precipitating hydrometeor paths; i.e., the rainwater path (RWP) and the snow water path (SWP), through pre-industrial (PI) to present-day (PD) changes in aerosols. The PD minus PI change (susceptibility) in RWP is highly correlated ($r = 0.59$) with that in CLWP (Fig. 3a). We interpret this strong correlation to be the result of the close co-variance of cloud and rainwater through aerosol perturbations, with the cloud water being a direct source of the rainwater. The PD minus PI change in SWP is also positively correlated, though weaker ($r = 0.39$), than that in CLWP (Fig. 3b), suggesting that precipitating snow also co-varies with cloud water through aerosol perturbations. Given that SWP is significantly larger than RWP in our model (Fig. S2; see also Michibata et al. (2019)), and that snowflakes, with residence times longer than those of rain, are more likely to interact with clouds, the increased CLWP caused by anthropogenic aerosols can act as an efficient source of snow via interactions among cloud droplets and snowflakes (e.g., riming), likely resulting in the evident robust positive relationship.

These positive correlations between precipitating hydrometeors and cloud water suggest that aerosol-induced increases in ~~the water mass suspended in the atmosphere~~ cloud mass are caused, in part, by increases of rain and snow in PROG, in contrast to those caused by increases of cloud water and ice alone in DIAG. Given that raindrops and snowflakes are optically much thinner in the SW spectrum than cloud droplets and ice crystals, respectively, increases of precipitating hydrometeors can explain both the stronger $\mathrm{ERF}_{\mathrm{aci}}^{\mathrm{LW}}$ and weaker $\mathrm{ERF}_{\mathrm{aci}}^{\mathrm{SW}}$ in PROG compared with DIAG (Figs. 1 and 2). Furthermore, falling snow is more

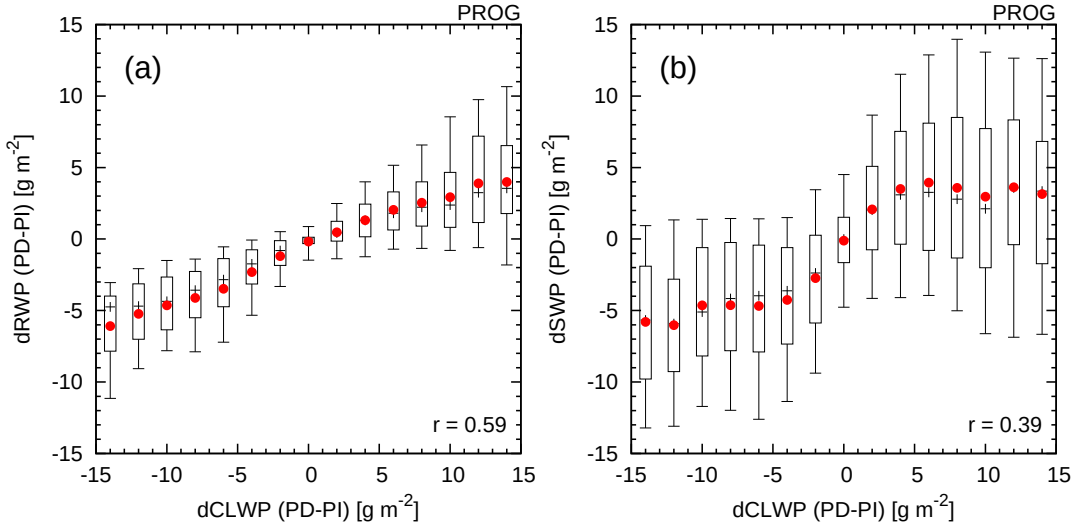


**Figure 3.** Relationship between the change in annual mean CLWP and that in annual mean **(a)** RWP and **(b)** SWP, from the change in aerosols from PI to PD conditions, simulated using the PROG scheme. Box-whisker plots represent the 10th, 25th, 50th (black "+"), 75th, and 90th percentiles of the data within each bin based on the annual mean. Plots in red show the mean. The correlation coefficient ($r$) is given in the figure.

likely to deplete underlying cloud droplets in PROG, with its explicit representation of the riming process, which can lead to a reduction of cloud water susceptibility to aerosols. This proposed mechanism can also explain the systematic change in the geographical distribution of $\mathrm{ERF_{aci}}$ between DIAG and PROG (Fig. 1). Indeed, regions with a significant reduction in $\mathrm{ERF_{aci}}$ (i.e., over East Asia, Europe, and North America) correspond well to those with large values of SWP (Fig. S3), where the PD – PI increase in CLWP is also reduced significantly (Fig. S4). These results lend further credence to the hypothesis of snow-induced buffering of ACI in our model.

The buffering process, via interactions among hydrometeors described above, depends strongly on the fundamental uncertainty in model representations of various microphysical processes. We therefore now further explore how $\mathrm{ERF_{aci}}$ and its buffering by precipitation processes are sensitive to microphysical process representations as summarized in Fig. 4 (see also Sect. 2.2 for details of experiments). The processes examined here are the autoconversion of liquid droplets, the Wegener–Bergeron–Findeisen (WBF) process, the aggregation of ice crystals, riming, and ice nucleation by freezing aerosols, which are all important sources of uncertainty in GCMs (Lawson and Gettelman, 2014; Gettelman, 2015; Sant et al., 2015). As expected, the simulated $\mathrm{ERF_{aci}}$ is highly sensitive to the autoconversion scheme used, mainly because of its varying dependence on $N_c$ among the various schemes (Jing et al., 2019). ~~The potential change of $\mathrm{ERF_{aci}}$ from the default PROG scheme is up to 60%~~ Different liquid autoconversion scheme with PROG can change $\mathrm{ERF_{aci}}$ by 39%, from $-18\%$ to $+21\%$ (blue bars in Fig. 4). The impacts of the autoconversion scheme on $\mathrm{ERF_{aci}}$, however, are smaller than those of the treatment of rain and snow (ca. ~~75%~~54% change).

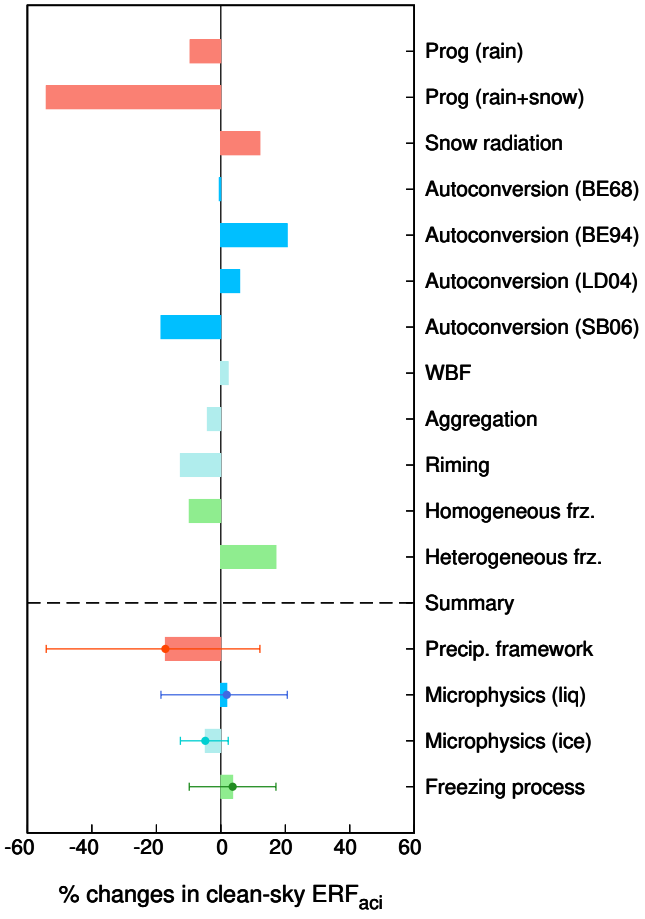


**Figure 4.** Percentage change of global annual mean clean-sky $\mathrm{ERF_{aci}}$ in response to (red) the precipitation treatment, (blue) liquid microphysics, (cyan) ice microphysics, and (green) nucleation of new ice particles due to freezing. Error bars represent the minimum and maximum range for each component considered in this study.

The mixed- and ice-phase processes (WBF, aggregation, and riming), represented more explicitly with a larger degree of freedom in PROG than in DIAG, ~~are all found to reduce~~ ~~$\mathrm{ERF_{aci}}$~~ can change $\mathrm{ERF_{aci}}$ by 15%, from ~~4% to 36%~~ −13% to +2% (cyan bars in Fig. 4). Among the mixed- and ice-phase microphysics processes, the process found to most influence $\mathrm{ERF_{aci}}$ is the riming of cloud droplets on snow, supporting the hypothesized mechanism of snow-induced buffering of ACI discussed above. The magnitude of $\mathrm{ERF_{aci}}$ is sensitive to ice nucleation processes as well (green bars in Fig. 4), because the change in ice number concentration directly controls the size of the crystals and thus the conversion timescale from ice to snow in our model. Although the $\mathrm{ERF_{aci}}$ variations with changing liquid and ice microphysical processes do not reach the difference of $\mathrm{ERF_{aci}}$ between the DIAG and PROG (i.e., 54%), both wet-scavenging of aerosols and coalescence scavenging of cloud droplets also contribute to the ACI reduction (McCoy et al., 2020) due to the accretion-driven buffering mechanisms (Michibata and Suzuki, 2020), which should explain the remaining part of the $\mathrm{ERF_{aci}}$ difference.

In summary, we found that the treatment of precipitation (PROG vs DIAG) is the most influential factor controlling $\mathrm{ERF_{aci}}$ (red bars in Fig. 4) among all of the "tunable knobs" associated with the various microphysical processes in our model. It should also be emphasized that the $\mathrm{ERF_{aci}}$ change caused by the precipitation treatment (ca. ~~75%~~54% in magnitude), absent from previous climate modeling studies, has the potential to resolve some of the differences between satellite estimates of $\mathrm{ERF_{aci}}$ (Bellouin et al., 2013; Chen et al., 2014; Christensen et al., 2017) and GCMs (Shindell et al., 2013; Zelinka et al., 2014; Heyn et al., 2017). These findings need to be tested further using other GCMs as they incorporate prognostic precipitation in future studies.

## 5 Summary and future work

In this study, the sensitivities of $\mathrm{ERF_{aci}}$ to various treatments of precipitation and microphysical process representations in a GCM have been systematically examined. As few GCMs incorporate explicit representations of two-moment prognostic precipitation with the radiative effects of precipitating hydrometeors (~~currently available only in~~ e.g., CAM6 MG2/MG3 (Gettelman et al., 2015, 2019), E3SM (Rasch et al., 2019), GISS-E3, and MIROC6 CHIMERRA (Michibata et al., 2019)), we used a single model framework to evaluate the sensitivities. This also allowed us to avoid uncertainties from inter-model differences in parameterizations other than the targeted processes.

We found that the treatment of precipitation in GCMs (PROG vs DIAG) has a significant impact on the magnitude of $\mathrm{ERF_{aci}}$ (Figs. 1 and 2), which we interpret to be driven mainly by collection processes among precipitating snow and cloud droplets (i.e., riming). As the SWP is more than twice as large as the RWP in our PROG model, and is in good agreement with satellite retrievals (Michibata et al., 2019), falling snowflakes efficiently accrete and deplete the underlying cloud water thus partly cancelling the CLWP response to aerosols. Changes in RWP and SWP though PI to PD aerosol perturbations were also positively correlated with that in CLWP (Fig. 3), suggesting that snow can co-exist with cloud water to a degree sufficient to buffer the cloud water response to aerosol perturbations (Fig. 4). The signatures of the snow-induced buffering are also found geographically over regions with significant reductions in $\mathrm{ERF_{aci}}$ (e.g., East Asia, Europe, and North America) that correspond closely to regions with particularly large SWP (Figs. 1 and S3). Sets of sensitivity experiments, performed both with and without snow radiative effects, did not reveal a significant difference in $\mathrm{ERF_{aci}}$ as a result of the near cancellation of SW and LW changes caused by snow. This means that the prognostic treatment of precipitation itself is critical for the buffering of ACI. Accordingly, the impact of a prognostic treatment of precipitation on the magnitude of $\mathrm{ERF_{aci}}$ was greater than changes to any of the other "tunable knobs" inherent to the various microphysical processes (e.g., autoconversion, ice microphysics, and ice nucleation). Notably, precipitation-driven buffering effects (ca. ~~75%~~54% change in $\mathrm{ERF_{aci}}$) can broadly explain the current model-observation discrepancy in estimated $\mathrm{ERF_{aci}}$ (Boucher et al., 2013; Lohmann, 2017).

However, the results presented here are based on a single GCM framework and need to be replicated using other GCMs as they incorporate prognostic precipitation frameworks in the future (Li et al., 2020). This is particularly true because little is known about aerosol influences on mixed- and ice-phase clouds as well as deep convective clouds (Rosenfeld et al., 2014; Fan et al., 2018) and cirrus clouds (Penner et al., 2018) at a fundamental process-level, and the degree of microphysical

complexity differs widely among GCMs (Heyn et al., 2017). Although the responses of clouds and precipitation to aerosol perturbations are therefore likely to be model dependent, the sign of the response of $\mathrm{ERF_{aci}}$ to the precipitation framework and microphysical processes is consistent with a previous assessment using CAM5/MG2 (Gettelman, 2015), suggesting that the major findings of this study will apply across the models. Thus, it is left for important future studies to quantify the inter-model spread of $\mathrm{ERF_{aci}}$ sensitivity to microphysical processes and their interplay with precipitation processes as more GCMs begin to include prognostic precipitation. Furthermore, a theoretical approach (Glassmeier and Lohmann, 2016) and idealized process modeling (Glassmeier et al., 2019) are also required urgently to solidify the process-level understanding of snow-induced buffering hypothesis, which are our important future work beyond the present study.

This study primarily focused on $\mathrm{ERF_{aci}}$ sensitivities to the CLWP adjustment rather than cloud fraction adjustment, because aerosol effects are directly linked to the CLWP change through the modification of the mass conversion rate from cloud water to rainwater that itself relates to the treatment of precipitation (i.e., DIAG vs PROG). However, it is important in future studies to separating the ACI into the Twomey forcing and rapid adjustments of CLWP and cloud fraction (e.g., Goren and Rosenfeld, 2014; Mülmenstädt et al., 2019) for better understanding how the treatment of precipitation influences micro- and macroscopic cloud properties (Michibata and Suzuki, 2020), which relates to the fundamental inter-model spread in $\mathrm{ERF_{aci}}$ (Gryspeerdt et al., 2020; Bellouin et al., 2020).

*Data availability.* The results of the MIROC-SPRINTARS simulations used to produce the figures can be obtained from the corresponding author upon reasonable request.

*Author contributions.* TM designed research; TM, KS, and TT performed research; TM analyzed data; and TM and KS wrote the paper.

*Competing interests.* The authors declare that they have no conflict of interest.

*Acknowledgements.* The authors would like to thank the developers of both SPRINTARS and MIROC. The new microphysics and radiation schemes were optimized by Koji Ogochi. Simulations by MIROC-SPRINTARS were executed on the SX-ACE supercomputer system of the National Institute for Environmental Studies, Japan. This study was supported by JSPS KAKENHI Grant Numbers JP18J00301, JP19K14795, and JP19H05669; the Environment Research and Technology Development Fund (JPMEERF20202R03) of the Environmental Restoration and Conservation Agency of Japan; the Integrated Research Program for Advancing Climate Models (TOUGOU) Grant Number JPMXD0717935457 from the Ministry of Education, Culture, Sports, Science and Technology (MEXT); and the Collaborative Research Program of the Research Institute for Applied Mechanics, Kyushu University. The authors are grateful to Johannes Mülmenstädt (Pacific Northwest National Laboratory) and one anonymous reviewer for providing constructive suggestions and comments, that helped to improve the manuscript.

## References


Abdul-Razzak, H. and Ghan, J.: A parameterization of aerosol activation 2. Multiple aerosol types, Journal of Geophysical Research, 105, 6837–6844, 2000.

Albrecht, B. A.: Aerosols, cloud microphysics, and fractional cloudiness, Science, 245, 1227–1230, 1989.

Beheng, K. D.: A parameterization of warm cloud microphysical conversion processes, Atmospheric Research, 33, 193–206, 1994.

Bellouin, N., Quaas, J., Morcrette, J. J., and Boucher, O.: Estimates of aerosol radiative forcing from the MACC re-analysis, Atmospheric Chemistry and Physics, 13, 2045–2062, https://doi.org/10.5194/acp-13-2045-2013, 2013.

Bellouin, N., Quaas, J., Gryspeerdt, E., Kinne, S., Stier, P., Watson-Parris, D., Boucher, O., Carslaw, K., Christensen, M., Daniau, A., Dufresne, J., Feingold, G., Fiedler, S., Forster, P., Gettelman, A., Haywood, J., Lohmann, U., Malavelle, F., Mauritsen, T., McCoy, D., Myhre, G., Mülmenstädt, J., Neubauer, D., Possner, A., Rugenstein, M., Sato, Y., Schulz, M., Schwartz, S., Sourdeval, O., Storelvmo, T., Toll, V., Winker, D., and Stevens, B.: Bounding global aerosol radiative forcing of climate change, Reviews of Geophysics, 58, e2019RG000 660, https://doi.org/10.1029/2019rg000660, 2020.

Bergeron, T.: On the physics of cloud and precipitation, in: Proces Verbaux de l'Association de Meteorologie, Intl. Union of Geod. and Geophys., Paris., pp. 156–178, 1935.

Berry, E. X.: Modification of the Warm Rain Process, in: Proc. First Conf. on Weather Modification, pp. 81–85, Albany, NY. Amer. Meteor. Soc, paper presented at 1st National Conf. on Weather Modification, April 28–May 1, 1968.

Boucher, O., Randall, D., Artaxo, P., Bretherton, C., Feingold, G., Forster, P., Kerminen, V.-M., Kondo, Y., Liao, H., Lohmann, U., Rasch, P., Satheesh, S. K., Sherwood, S., Stevens, B., and Zhang, X. Y.: Clouds and aerosols, pp. 571–657, Cambridge University Press, Cambridge, UK, https://doi.org/10.1017/CBO9781107415324.016, 2013.

Chen, Y.-C., Christensen, M. W., Stephens, G. L., and Seinfeld, J. H.: Satellite-based estimate of global aerosol-cloud radiative forcing by marine warm clouds, Nature Geosci, 7, 643–646, 2014.

Chepfer, H., Bony, S., Winker, D., Cesana, G., Dufresne, J. L., Minnis, P., Stubenrauch, C. J., and Zeng, S.: The GCM-oriented CALIPSO cloud product (CALIPSO-GOCCP), Journal of Geophysical Research: Atmospheres, 115, D00H16, https://doi.org/10.1029/2009JD012251, 2010.

Christensen, M. W., Chen, Y. C., and Stephens, G. L.: Aerosol indirect effect dictated by liquid clouds, Journal of Geophysical Research, 121, 14 636–14 650, https://doi.org/10.1002/2016JD025245, 2016.

Christensen, W. M., Neubauer, D., Poulsen, A. C., Thomas, E. G., McGarragh, R. G., Povey, C. A., Proud, R. S., and Grainger, G. R.: Unveiling aerosol–cloud interactions – Part 1: Cloud contamination in satellite products enhances the aerosol indirect forcing estimate, Atmospheric Chemistry and Physics, 17, 13 151–13 164, https://doi.org/10.5194/acp-17-13151-2017, 2017.

Douglas, A. and L'Ecuyer, T.: Quantifying cloud adjustments and the radiative forcing due to aerosol-cloud interactions in satellite observations of warm marine clouds, Atmospheric Chemistry and Physics, 20, 6225–6241, 2020.

Fan, J., Zhang, Y., Yang, Y., Comstock, J. M., Feng, Z., Gao, W., Mei, F., Rosenfeld, D., Li, Z., Giangrande, S. E., Wang, J., Machado, L. A., Braga, R. C., Martin, S. T., Artaxo, P., Barbosa, H. M., Gomes, H. B., Pöhlker, C., Pöhlker, M. L., Pöschl, U., and De Souza, R. A.: Substantial convection and precipitation enhancements by ultrafine aerosol particles, Science, 359, 411–418, https://doi.org/10.1126/science.aan8461, 2018.

Findeisen, Z.: Kolloid-meteorologische Vorgange bei Neiderschlags-bildung, Meteorol Z., 55, 121–133, 1938.

Gettelman, A.: Putting the clouds back in aerosol–cloud interactions, Atmospheric Chemistry and Physics, 15, 12 397–12 411, https://doi.org/10.5194/acp-15-12397-2015, 2015.

Gettelman, A., Morrison, H., Terai, C. R., and Wood, R.: Microphysical process rates and global aerosol–cloud interactions, Atmos. Chem. Phys., 13, 9855–9867, https://doi.org/10.5194/acp-13-9855-2013, 2013.

Gettelman, A., Morrison, H., Santos, S., Bogenschutz, P., and Caldwell, P. M.: Advanced two-moment bulk microphysics for global models. Part II: Global model solutions and aerosol–cloud interactions, Journal of Climate, 28, 1288–1307, https://doi.org/10.1175/JCLI-D-14-00103.1, 2015.

Gettelman, A., Morrison, H., Thayer-Calder, K., and Zarzycki, C. M.: The Impact of Rimed Ice Hydrometeors on Global and Regional Climate, Journal of Advances in Modeling Earth Systems, 11, https://doi.org/10.1029/2018MS001488, 2019.

Ghan, S., Wang, M., Zhang, S., Ferrachat, S., Gettelman, A., Griesfeller, J., Kipling, Z., Lohmann, U., Morrison, H., Neubauer, D., Partridge, D. G., Stier, P., Takemura, T., Wang, H., and Zhang, K.: Challenges in constraining anthropogenic aerosol effects on cloud radiative forcing using present-day spatiotemporal variability, Proceedings of the National Academy of Sciences, p. 201514036, https://doi.org/10.1073/pnas.1514036113, 2016.

Ghan, S. J.: Technical note: Estimating aerosol effects on cloud radiative forcing, Atmospheric Chemistry and Physics, 13, 9971–9974, https://doi.org/10.5194/acp-13-9971-2013, 2013.

Glassmeier, F. and Lohmann, U.: Constraining precipitation susceptibility of warm, ice- and mixed-phase clouds with microphysical equations, Journal of the Atmospheric Sciences, 73, 5003–5023, https://doi.org/10.1175/JAS-D-16-0008.1, 2016.

Glassmeier, F., Hoffmann, F., Johnson, J. S., Yamaguchi, T., Carslaw, K. S., and Feingold, G.: An emulator approach to stratocumulus susceptibility, Atmospheric Chemistry and Physics, 19, 10 191–10 203, https://doi.org/10.5194/acp-19-10191-2019, 2019.

Goren, T. and Rosenfeld, D.: Decomposing aerosol cloud radiative effects into cloud cover, liquid water path and Twomey components in marine stratocumulus, Atmospheric Research, 138, 378–393, https://doi.org/10.1016/j.atmosres.2013.12.008, 2014.

Grandey, B. S., Rothenberg, D., Avramov, A., Jin, Q., Lee, H. H., Liu, X., Lu, Z., Albani, S., and Wang, C.: Effective radiative forcing in the aerosol-climate model CAM5.3-MARC-ARG, Atmospheric Chemistry and Physics, 18, 15 783–15 810, https://doi.org/10.5194/acp-18-15783-2018, 2018.

Gryspeerdt, E., Goren, T., Sourdeval, O., Quaas, J., Mülmenstädt, J., Dipu, S., Unglaub, C., Gettelman, A., and Christensen, M.: Constraining the aerosol influence on cloud liquid water path, Atmospheric Chemistry and Physics, 19, 5331–5347, https://doi.org/10.5194/acp-19-5531-2019, 2019.

Gryspeerdt, E., Mülmenstädt, J., Gettelman, A., Malavelle, F. F., Morrison, H., Neubauer, D., Partridge, D. G., Stier, P., Takemura, T., Wang, H., Wang, M., and Zhang, K.: Surprising similarities in model and observational aerosol radiative forcing estimates, Atmospheric Chemistry and Physics, 20, 613–623, https://doi.org/10.5194/acp-20-613-2020, 2020.

Heyn, I., Block, K., Mülmenstädt, J., Gryspeerdt, E., Kühne, P., Salzmann, M., and Quaas, J.: Assessment of simulated aerosol effective radiative forcings in the terrestrial spectrum, Geophysical Research Letters, 44, 1001–1007, https://doi.org/10.1002/2016GL071975, 2017.

Jing, X., Suzuki, K., and Michibata, T.: The Key Role of Warm Rain Parameterization in Determining the Aerosol Indirect Effect in a Global Climate Model, Journal of Climate, 32, 4409–4430, https://doi.org/10.1175/jcli-d-18-0789.1, 2019.

Khairoutdinov, M. and Kogan, Y.: A new cloud physics parameterization in a large-eddy simulation model of marine stratocumulus., Monthly Weather Review, 128, 229–243, 2000.

Lawson, R. P. and Gettelman, A.: Impact of Antarctic mixed-phase clouds on climate, Proceedings of the National Academy of Sciences, 111, 18 156–18 161, https://doi.org/10.1073/pnas.1418197111, 2014.

Lebo, Z. J. and Feingold, G.: On the relationship between responses in cloud water and precipitation to changes in aerosol, Atmos. Chem. Phys., 14, 11 817–11 831, https://doi.org/10.5194/acp-14-11817-2014, 2014.

Li, J. F., Xu, K., Jiang, J. H., Lee, W., Wang, L., Yu, J., Stephens, G., Fetzer, E., and Wang, Y.: An Overview of CMIP5 and CMIP6 Simulated Cloud Ice, Radiation Fields, Surface Wind Stress, Sea Surface Temperatures, and Precipitation Over Tropical and Subtropical Oceans, Journal of Geophysical Research: Atmospheres, 125, e2020JD032 848, https://doi.org/10.1029/2020jd032848, 2020.

Li, J.-L. F., Lee, W.-L., Waliser, D. E., Neelin, J. D., Stachnik, J. P., and Lee, T.: Cloud-precipitation-radiation-dynamics interaction in global climate models: A snow and radiation interaction sensitivity experiment, Journal of Geophysical Research: Atmospheres, 119, 3809–3824, https://doi.org/10.1002/2013JD021038, 2014.

Liu, Y. and Daum, P. H.: Parameterization of the autoconversion process. Part I: Analytical formulation of the Kessler-type parameterizations., Journal of the Atmospheric Sciences, 61, 1539–1548, https://doi.org/10.1175/1520-0469(2004)061<1539:POTAPI>2.0.CO;2, 2004.

Lohmann, U.: Anthropogenic Aerosol Influences on Mixed-Phase Clouds, Current Climate Change Reports, 3, 32–44, https://doi.org/10.1007/s40641-017-0059-9, 2017.

Lohmann, U. and Hoose, C.: Sensitivity studies of different aerosol indirect effects in mixed-phase clouds, Atmospheric Chemistry and Physics, 9, 8917–8934, https://doi.org/10.5194/acp-9-8917-2009, 2009.

Ma, P. L., Rasch, P. J., Chepfer, H., Winker, D. M., and Ghan, S. J.: Observational constraint on cloud susceptibility weakened by aerosol retrieval limitations, Nature Communications, 9, 2640, https://doi.org/10.1038/s41467-018-05028-4, 2018.

Malavelle, F. F., Haywood, J. M., Jones, A., Gettelman, A., Clarisse, L., Bauduin, S., Allan, R. P., Karset, I. H. H., Kristjánsson, J. E., Oreopoulos, L., Cho, N., Lee, D., Bellouin, N., Boucher, O., Grosvenor, D. P., Carslaw, K. S., Dhomse, S., Mann, G. W., Schmidt, A., Coe, H., Hartley, M. E., Dalvi, M., Hill, A. A., Johnson, B. T., Johnson, C. E., Knight, J. R., O'Connor, F. M., Partridge, D. G., Stier, P., Myhre, G., Platnick, S., Stephens, G. L., Takahashi, H., and Thordarson, T.: Strong constraints on aerosol–cloud interactions from volcanic eruptions, Nature, 546, 485–491, https://doi.org/10.1038/nature22974, 2017.

McCoy, D., Field, P., Gordon, H., Elsaesser, G., and Grosvenor, D.: Untangling causality in midlatitude aerosol-cloud adjustments, Atmospheric Chemistry and Physics, 20, 4085–4103, https://doi.org/10.5194/acp-20-4085-2020, 2020.

Michibata, T. and Suzuki, K.: Reconciling compensating errors between precipitation constraints and the energy budget in a climate model, Geophysical Research Letters, 47, e2020GL088 340, https://doi.org/10.1029/2020GL088340, 2020.

Michibata, T. and Takemura, T.: Evaluation of autoconversion schemes in a single model framework with satellite observations, Journal of Geophysical Research, 120, 9570–9590, https://doi.org/10.1002/2015JD023818, 2015.

Michibata, T., Suzuki, K., Sato, Y., and Takemura, T.: The source of discrepancies in aerosol–cloud–precipitation interactions between GCM and A-Train retrievals, Atmospheric Chemistry and Physics, 16, 15 413–15 424, https://doi.org/10.5194/acp-16-15413-2016, 2016.

Michibata, T., Suzuki, K., Sekiguchi, M., and Takemura, T.: Prognostic Precipitation in the MIROC6-SPRINTARS GCM: Description and Evaluation against Satellite Observations, Journal of Advances in Modeling Earth Systems, 11, 839–860, https://doi.org/10.1029/2018MS001596, 2019.

Mülmenstädt, J. and Feingold, G.: The Radiative Forcing of Aerosol–Cloud Interactions in Liquid Clouds: Wrestling and Embracing Uncertainty, Current Climate Change Reports, 4, 23–40, https://doi.org/10.1007/s40641-018-0089-y, 2018.

Mülmenstädt, J., Gryspeerdt, E., Salzmann, M., Ma, P.-L., Dipu, S., and Quaas, J.: Separating radiative forcing by aerosol–cloud interactions and fast cloud adjustments in the ECHAM-HAMMOZ aerosol–climate model using the method of partial radiative perturbations, Atmospheric Chemistry and Physics, pp. 15 415–15 429, https://doi.org/10.5194/acp-19-15415, 2019.

Mülmenstädt, J., Nam, C., Salzmann, M., Kretzschmar, J., Ecuyer, T. S. L., Lohmann, U., Ma, P.-l., Myhre, G., Neubauer, D., Stier, P., Suzuki, K., Wang, M., and Quaas, J.: Reducing the aerosol forcing uncertainty using observational constraints on warm rain processes, Science Advances, 6, eaaz6433, https://doi.org/10.1126/sciadv.aaz6433, 2020.

Penner, J. E., Zhou, C., Garnier, A., and Mitchell, D. L.: Anthropogenic aerosol indirect effects in cirrus clouds, Journal of Geophysical Research: Atmospheres, 123, 11 652–11 677, https://doi.org/10.1029/2018JD029204, 2018.

Posselt, R. and Lohmann, U.: Introduction of prognostic rain in ECHAM5: design and single column model simulations, Atmospheric Chemistry and Physics, 8, 2949–2963, https://doi.org/10.5194/acp-8-2949-2008, 2008.

Quaas, J., Ming, Y., Menon, S., Takemura, T., Wang, M., Penner, J. E., Gettelman, A., Lohmann, U., Bellouin, N., Boucher, O., Sayer, A. M., Thomas, G. E., McComiskey, A., Feingold, G., Hoose, C., Kristjánsson, J. E., Liu, X., Balkanski, Y., Donner, L. J., Ginoux, P. A., Stier, P., Feichter, J., Sednev, I., Bauer, S. E., Koch, D., Grainger, R. G., Kirkevåg, A., Iversen, T., Seland, Ø., Easter, R., Ghan, S. J., Rasch, P. J., Morrison, H., Lamarque, J.-F., Iacono, M. J., Kinne, S., and Schulz, M.: Aerosol indirect effects – general circulation model intercomparison and evaluation with satellite data, Atmospheric Chemistry and Physics, 9, 8697–8717, https://doi.org/10.5194/acp-9-8697-2009, 2009.

Rasch, P. J., Xie, S., Ma, P., Lin, W., Wang, H., Tang, Q., Burrows, S. M., Caldwell, P., Zhang, K., Easter, R. C., Cameron-Smith, P., Singh, B., Wan, H., Golaz, J., Harrop, B. E., Roesler, E., Bacmeister, J., Larson, V. E., Evans, K. J., Qian, Y., Taylor, M., Leung, L. R., Zhang, Y., Brent, L., Branstetter, M., Hannay, C., Mahajan, S., Mametjanov, A., Neale, R., Richter, J. H., Yoon, J., Zender, C. S., Bader, D., Flanner, M., Foucar, J. G., Jacob, R., Keen, N., Klein, S. A., Liu, X., Salinger, A., Shrivastava, M., and Yang, Y.: An Overview of the Atmospheric Component of the Energy Exascale Earth System Model, Journal of Advances in Modeling Earth Systems, 11, 2377–2411, https://doi.org/10.1029/2019ms001629, 2019.

Rosenfeld, D., Sherwood, S., Wood, R., and Donner, L.: Climate effects of aerosol-cloud interactions, Science, 343, 379–380, 2014.

Rosenfeld, D., Zhu, Y., Minghuai, W., Zheng, Y., Goren, T., and Yu, S.: Aerosol-driven droplet concentrations dominate converage and water of oceanic low level clouds, Science, 363, 599, https://doi.org/10.1126/science.aav0566, 2019.

Sant, V., Posselt, R., and Lohmann, U.: Prognostic precipitation with three liquid water classes in the ECHAM5–HAM GCM, Atmospheric Chemistry and Physics, 15, 8717–8738, https://doi.org/10.5194/acp-15-8717-2015, 2015.

Seifert, A. and Beheng, K. D.: A two-moment cloud microphysics parameterization for mixed-phase clouds. Part 1: Model description, Meteorology and Atmospheric Physics, 92, 45–66, https://doi.org/10.1007/s00703-005-0112-4, 2006.

Seifert, A., Heus, T., Pincus, R., and Stevens, B.: Large-eddy simulation of the transient and near-equilibrium behavior of precipitating shallow convection, Journal of Advances in Modeling Earth Systems, 7, https://doi.org/10.1002/ 2015MS000489, 2015.

Seinfeld, J. H., Bretherton, C., Carslaw, K. S., Coe, H., DeMott, P. J., Dunlea, E. J., Feingold, G., Ghan, S., Guenther, A. B., Kahn, R., Kraucunas, I., Kreidenweis, S. M., Molina, M. J., Nenes, A., Penner, J. E., Prather, K. A., Ramanathan, V., Ramaswamy, V., Rasch, P. J., Ravishankara, A. R., Rosenfeld, D., Stephens, G., and Wood, R.: Improving our fundamental understanding of the role of aerosol–cloud interactions in the climate system, Proceedings of the National Academy of Sciences, 113, 5781–5790, https://doi.org/10.1073/pnas.1514043113, 2016.

Shindell, D. T., Lamarque, J. F., Schulz, M., Flanner, M., Jiao, C., Chin, M., Young, P. J., Lee, Y. H., Rotstayn, L., Mahowald, N., Milly, G., Faluvegi, G., Balkanski, Y., Collins, W. J., Conley, A. J., Dalsoren, S., Easter, R., Ghan, S., Horowitz, L., Liu, X., Myhre, G., Nagashima, T., Naik, V., Rumbold, S. T., Skeie, R., Sudo, K., Szopa, S., Takemura, T., Voulgarakis, A., Yoon, J. H., and Lo, F.: Radiative forcing in the ACCMIP historical and future climate simulations, Atmospheric Chemistry and Physics, 13, 2939–2974, https://doi.org/10.5194/acp-13-2939-2013, 2013.

Stevens, B. and Feingold, G.: Untangling aerosol effects on clouds and precipitation in a buffered system, Nature, 461, 607–613, https://doi.org/10.1038/nature08281, 2009.

Swales, D. J., Pincus, R., and Bodas-Salcedo, A.: The Cloud Feedback Model Intercomparison Project Observational Simulator Package: Version 2, Geoscientific Model Development, 11, 77–81, https://doi.org/10.5194/gmd-11-77-2018, 2018.

Takemura, T., Egashira, M., Matsuzawa, K., Ichijo, H., O'ishi, R., and Abe-Ouchi, a.: A simulation of the global distribution and radiative forcing of soil dust aerosols at the Last Glacial Maximum, Atmospheric Chemistry and Physics, 9, 3061–3073, https://doi.org/10.5194/acp-9-3061-2009, 2009.

Tatebe, H., Ogura, T., Nitta, T., Komuro, Y., Ogochi, K., Takemura, T., Sudo, K., Sekiguchi, M., Abe, M., Saito, F., Chikira, M., Watanabe, S., Mori, M., Hirota, N., Kawatani, Y., Mochizuki, T., Yoshimura, K., Takata, K., O'ishi, R., Yamazaki, D., Suzuki, T., Kurogi, M., Kataoka, T., Watanabe, M., and Kimoto, M.: Description and basic evaluation of simulated mean state, internal variability, and climate sensitivity in MIROC6, Geoscientific Model Development, 12, 2727–2765, https://doi.org/10.5194/gmd-12-2727-2019, 2019.

Toll, V., Christensen, M., Quaas, J., and Bellouin, N.: Weak average liquid-cloud-water response to anthropogenic aerosols, Nature, 572, 51–55, https://doi.org/10.1038/s41586-019-1423-9, 2019.

Twomey, S.: The influence of pollution on the shortwave albedo of clouds, Journal of the Atmospheric Sciences, 34, 1149–1152, 1977.

Waliser, D. E., Li, J. L. F., L'Ecuyer, T. S., and Chen, W. T.: The impact of precipitating ice and snow on the radiation balance in global climate models, Geophysical Research Letters, 38, L06 802, https://doi.org/10.1029/2010GL046478, 2011.

Wang, M., Ghan, S., Ovchinnikov, M., Liu, X., Easter, R., Kassianov, E., Qian, Y., and Morrison, H.: Aerosol indirect effects in a multi-scale aerosol-climate model PNNL-MMF, Atmospheric Chemistry and Physics, 11, 5431–5455, https://doi.org/10.5194/acp-11-5431-2011, 2011.

Wang, M., Ghan, S., Liu, X., L'Ecuyer, T. S., Zhang, K., Morrison, H., Ovchinnikov, M., Easter, R., Marchand, R., Chand, D., Qian, Y., and Penner, J. E.: Constraining cloud lifetime effects of aerosols using A-Train satellite observations, Geophysical Research Letters, 39, L15 709, https://doi.org/10.1029/2012GL052204, 2012.

Watanabe, M., Emori, S., Satoh, M., and Miura, H.: A PDF-based hybrid prognostic cloud scheme for general circulation models, Climate Dynamics, 33, 795–816, https://doi.org/10.1007/s00382-008-0489-0, 2009.

Wegener, A.: Thermodynamik der atmosphäre, J. A. Barth, 1911.

Wilson, D. R. and Ballard, S. P.: A microphysically based precipitation scheme for the UK Meteorological Office Unified Model, Quarterly Journal of the Royal Meteorological Society, 125, 1607–1636, https://doi.org/10.1256/smsqj.55706, 1999.

Wood, R.: Stratocumulus Clouds, Monthly Weather Review, 140, 2373–2423, https://doi.org/10.1175/MWR-D-11-00121.1, 2012.

Yang, P., Bi, L., Baum, B. A., Liou, K.-N., Kattawar, G. W., Mishchenko, M. I., and Cole, B.: Spectrally Consistent Scattering, Absorption, and Polarization Properties of Atmospheric Ice Crystals at Wavelengths from 0.2 to 100 $\mu$m, Journal of the Atmospheric Sciences, 70, 330–347, https://doi.org/10.1175/JAS-D-12-039.1, 2013.

Zelinka, M. D., Andrews, T., Forster, P. M., and Taylor, K. E.: Quantifying components of aerosol-cloud-radiation interactions in climate models, Journal of Geophysical Research, 119, 7599–7615, https://doi.org/10.1002/2014JD021710., 2014.

Zhang, S., Wang, M., Ghan, S. J., Ding, A., Wang, H., Zhang, K., Neubauer, D., Lohmann, U., Ferrachat, S., Takeamura, T., Gettelman, A., Morrison, H., Lee, Y. H., Shindell, D. T., Partridge, D. G., Stier, P., Kipling, Z., and Fu, C.: On the characteristics of aerosol indirect effect based on dynamic regimes in global climate models, Atmospheric Chemistry and Physics, 16, 2765–2783, https://doi.org/10.5194/acp-16-2765-2016, 2016.